

INFORMATION TO USERS

This manuscript has been reproduced from the microfilm master. UMI films the text directly from the original or copy submitted. Thus, some thesis and dissertation copies are in typewriter face, while others may be from any type of computer printer.

The quality of this reproduction is dependent upon the quality of the copy submitted. Broken or indistinct print, colored or poor quality illustrations and photographs, print bleedthrough, substandard margins, and improper alignment can adversely affect reproduction.

In the unlikely event that the author did not send UMI a complete manuscript and there are missing pages, these will be noted. Also, if unauthorized copyright material had to be removed, a note will indicate the deletion.

Oversize materials (e.g., maps, drawings, charts) are reproduced by sectioning the original, beginning at the upper left-hand corner and continuing from left to right in equal sections with small overlaps.

Photographs included in the original manuscript have been reproduced xerographically in this copy. Higher quality 6" x 9" black and white photographic prints are available for any photographs or illustrations appearing in this copy for an additional charge. Contact UMI directly to order.

**Bell & Howell Information and Learning
300 North Zeeb Road, Ann Arbor, MI 48106-1346 USA
800-521-0600**

UMI[®]

**A MODULAR APPROACH TO THE
SYNTHESIS OF QUICK-RETURN
MECHANISMS**

Chu-Jen Wu

Department of Mechanical Engineering
McGill University, Montreal

September 1998

A Thesis submitted to the Faculty of Graduate Studies and Research
in partial fulfilment of the requirements for the degree of
Master of Engineering

© CHU-JEN WU, MCMXCVIII



National Library
of Canada

Acquisitions and
Bibliographic Services

395 Wellington Street
Ottawa ON K1A 0N4
Canada

Bibliothèque nationale
du Canada

Acquisitions et
services bibliographiques

395, rue Wellington
Ottawa ON K1A 0N4
Canada

Your file Votre référence

Our file Notre référence

The author has granted a non-exclusive licence allowing the National Library of Canada to reproduce, loan, distribute or sell copies of this thesis in microform, paper or electronic formats.

The author retains ownership of the copyright in this thesis. Neither the thesis nor substantial extracts from it may be printed or otherwise reproduced without the author's permission.

L'auteur a accordé une licence non exclusive permettant à la Bibliothèque nationale du Canada de reproduire, prêter, distribuer ou vendre des copies de cette thèse sous la forme de microfiche/film, de reproduction sur papier ou sur format électronique.

L'auteur conserve la propriété du droit d'auteur qui protège cette thèse. Ni la thèse ni des extraits substantiels de celle-ci ne doivent être imprimés ou autrement reproduits sans son autorisation.

0-612-50676-2

ABSTRACT

Quick-return mechanisms are quite common in manufacturing processes, e.g. in pick-and-place operations, metal-cutting, and metal-forming, where dwell is usually required. Dwell is the period where a driven link remains stationary and the tool can be replaced or the workpiece can undergo a machining operation. Unlike lower-pair mechanisms, cam mechanisms can produce dwell exactly.

In this thesis, cam-follower systems are used as building modules in the design of quick-return mechanisms. The underlying cam mechanisms are optimized to obtain a compact, quick-return mechanism. A unified method for the optimization of cam mechanisms is proposed. The optimum parameters of the cam mechanism are obtained by cam-area minimization subject to performance and geometric constraints. In addition, the power required from the motor is reduced by adding an elastic torque-compensation mechanism to the system. A Graphical User Interface is developed to aid the designer during the design process.

The modular method is applied to the synthesis and optimization of long-stroke, quick-return mechanisms. In addition, the design of a simple cam mechanism to replace the transmission mechanism of a textile machine composed of an elliptic-gear train and a four-bar linkage is also included as an application example.

RÉSUMÉ

Les mécanismes de retour-rapide sont utilisés très fréquemment dans les procédés de fabrication, par exemple dans les opérations de transfert, de découpage et de poinçonnage. Habituellement, une période d'attente est nécessaire dans ce type d'opérations. L'attente est le temps où le lien mené reste stationnaire et l'outil peut être remplacé ou effectuer une opération d'usinage. Contrairement à des mécanismes plus simples, tels que les mécanismes à quatre barres, les systèmes à cames peuvent produire une période d'attente exacte.

Dans cette thèse, nous nous basons sur des mécanismes à cames pour la conception de mécanismes de retour-rapide. Les mécanismes à cames sont optimisés en utilisant une méthode unifiée pour obtenir un mécanisme de retour-rapide compact. Les paramètres optimaux sont obtenus en minimisant la taille de la came sujette aux contraintes géométriques et de performance. De plus, la puissance requise par le moteur est réduite par l'addition d'un système élastique pour compenser les variations de couple. Finalement, une interface graphique est développée pour aider l'utilisateur lors de la conception des mécanismes à cames.

Une méthodologie modulaire est appliquée à la synthèse et l'optimisation de mécanismes de retour-rapide à longue course utilisés dans la production de placage. Nous présentons également la conception d'un mécanisme à cames simple pour remplacer le mécanisme de transmission d'une machine textile composée d'un train d'engrenages elliptiques et d'un mécanisme à quatre barres.

ACKNOWLEDGEMENTS

I would like to thank my supervisor, Prof. Jorge Angeles, for his support, guidance, and suggestions during the course of my research. I am specially grateful for his careful review of the manuscript of the thesis.

Special thanks to my friend Oscar Navarro, who was always there to discuss different aspects of cam mechanisms. Many thanks to Pierre Montagnier for helping me produce the French translation of the abstract. Thanks are due to my colleagues at the Centre who shared with me their friendship, wise suggestions, and remarks.

I would also like to thank the Centre for Intelligent Machines of McGill University for providing state-of-the-art facilities and a pleasant research environment. Finally, I wish to thank my family and friends for their support and encouragement, which were essential for the completion of the work.

TABLE OF CONTENTS

ABSTRACT	ii
RÉSUMÉ	iii
ACKNOWLEDGEMENTS	iv
LIST OF FIGURES	vi
LIST OF TABLES	viii
CHAPTER 1. Introduction	1
1. Motivation	1
2. Literature Review	3
3. Lower-Pairs vs. Higher-Pair Mechanisms	4
CHAPTER 2. Kinematics of Cam Mechanisms and Problem Definition	5
1. Classification of Cam Mechanisms	5
1.1. Type of output motion	5
1.2. Relative layout of the instant screw axes	6
1.3. Follower configuration	6
2. The Displacement Program	7
3. Quick-Return Mechanisms	7
4. Long-Stroke, Quick-Return Mechanisms	10
5. Problem Definition	11
CHAPTER 3. Cam-Size Minimization Under Pressure-Angle Bounds	12

1. Pressure Angle	12
2. Determination of the Occurrence of the Maximum Pressure Angle	13
3. Translating Follower	14
4. Oscillating Follower	17
5. Graphical User Interface	19
CHAPTER 4. Optimization of the Elastic Torque Compensator	21
1. Nomenclature	21
2. Mechanism Dynamics and Mathematical Model	23
3. Selection of the Spring Constant	25
3.1. Lower Bound	25
3.2. Optimum Design of Helical Springs	27
CHAPTER 5. Applications	29
1. Design of a Long-Stroke Quick-Return Mechanism	29
1.1. Belt-Pulley mechanism	30
1.2. Ball Screws	38
2. Replacement of Elliptic Gears Using a Single Cam Mechanism	40
CHAPTER 6. Conclusions and Recommendations for Future Work	47
1. Conclusions	47
2. Recommendations for Future Work	48
References	49
APPENDIX A. Pitch Curve and Cam Profile	52

LIST OF FIGURES

1.1	Flow Chart for the design of mechanical systems	2
2.1	(a) Planar cam with offset knife-edge, translating follower: (b) planar cam with oscillating roller-follower.	6
2.2	Layout of the quick-return mechanism	8
2.3	Module of the quick-return mechanism	8
2.4	Relative layouts of the axes of the motor and the U-TSG: (a)co-axial, (b) parallel, and (c) intersecting	9
2.5	Modules of the modulating mechanism	9
2.6	Layout of the quick-return mechanism	11
3.1	Pressure angle of the translating follower	13
3.2	Knife-edge translating follower	15
3.3	Plot of the function defining the extremality condition of a translating quick-return cam mechanism. The dashed plot corresponds when $\alpha = \alpha_M$	16
3.4	Oscillating follower at lower dwell	18
3.5	Graphical user interface	19
4.1	The overall ETC system	22
4.2	Layout of (a) the primary system and (b) the ETC system	22

5.1	Quick-return motion	30
5.2	Velocity and acceleration of the quick-return motion	31
5.3	Pressure angle distribution for a belt-pulley mechanism	32
5.4	Profile of the minimum-size cam for the belt-pulley mechanism	32
5.5	Plot of the curvature	33
5.6	Fluctuating torque on the axis of the follower	34
5.7	Spectrum of the Fourier coefficients	35
5.8	Displacement of the spring for the optimum displacement program	36
5.9	Displacement of the spring: (a) optimum spring; (b) suboptimum spring	37
5.10	Cam profile of the ETC	37
5.11	3-D model of the modulating mechanism	38
5.12	Front view of the modulating mechanism	39
5.13	Fluctuating torque on the axis of the follower	40
5.14	Transmission mechanism of a textile machine.	41
5.15	Sketch of the elliptic-gear mechanism	41
5.16	Sketch of the four-bar mechanism	41
5.17	Input-output plots of the elliptic-gear train	43
5.18	Input-output plots of the four-bar linkage	44
5.19	Input-output plots of the composed mechanism	44
5.20	Pressure-angle distribution of the optimum cam	45
5.21	Profile of the optimum cam	46
A.1	Geometry of the cam profile.	53

LIST OF TABLES

2.1	Cam elements of the quick-return mechanism	10
2.2	Characteristics of the U-TSG	10
3.1	GUI functions	20
5.1	Quick-return motion	29
5.2	Parameters of the cam for the belt-pulley mechanism	30
5.3	Parameters of the cam	33
5.4	Parameters of the ETC cam	36
5.5	Parameters of the spring	38
5.6	Parameters of the transmission mechanism	42
5.7	Parameters of the optimum cam mechanism	45

CHAPTER 1

Introduction

A quick-return mechanism is a mechanical transmission that produces a slow feed motion under a load in one direction, followed by a fast return stroke under no load in the opposite direction. Quick-return mechanisms are quite common in manufacturing processes, e.g. in pick-and-place operations, metal-cutting, and metal-forming. A period of dwell is usually required in these types of operations. During dwell, the driven link remains stationary and the tool can be replaced or the workpiece can undergo a machining operation. Unlike lower-pair mechanisms, cam mechanisms can produce dwell exactly. Even with the introduction of servomechanisms, cam mechanisms are generally superior and more cost-effective. Servomechanisms are usually more expensive, and have low force and velocity characteristics as compared to cam mechanisms.

The design of quick-return mechanisms, like the design of mechanical systems at large can be broken down into several tasks, as depicted in Fig. 1.1: task definition, kinematic synthesis and dynamic analysis, optimization under geometric and mechanical constraints, and finally, simulation.

1. Motivation

The motion of the most common types of quick-return mechanisms is produced by a four-bar linkage, a six-bar linkage, or a Whitworth mechanism (Norton 1992). The

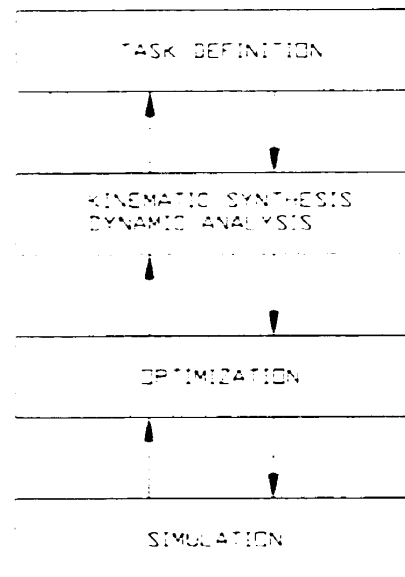


Figure 1.1: Flow Chart for the design of mechanical systems

problem with the use of linkages to produce a quick-return motion is that they cannot produce dwell exactly. Indeed, the input-output function of quick-return mechanisms with dwell is nonanalytic, while that of lower-pair mechanisms is analytic. Also, a large linkage is needed when the required stroke is large. One way to exactly reproduce the quick-return motion is to control the motor using a servocontroller, which has some disadvantages. First, the motor must accelerate and decelerate constantly, which may damage the motor. Another disadvantage is that usually a larger motor is required when the motor is not operated at constant velocity.

The main contribution of the thesis is the use of cam-follower systems as building modules in the design of quick-return mechanisms. Moreover, cam mechanisms are optimized to obtain a compact, quick-return mechanism, which is achieved by minimizing the cam size using a unified approach. For a cam-follower system, the input velocity is usually constant, but the required torque is periodic, by virtue of the inertia forces occurring because the velocity of the follower fluctuates periodically. A methodology to design and synthesize an elastic torque compensator to demodulate the periodic torque and render it constant is also proposed.

2. Literature Review

The study of the design of cam mechanism has attracted many researchers in recent years. The research has focused primarily on the selection of the displacement program (Erdman 1993), kinematic synthesis of cams (González-Palacios and Angeles 1993), and the dynamic analysis of cam mechanisms (Berzak 1982). The optimization of cam mechanisms has also been studied; it can be broken down into cam-size minimization (Angeles and López-Cajún 1991); vibration suppression (Tesar and Matthew 1976); and minimization of cam forces (Jones 1978) and stresses (Fenton 1975). This review focuses primarily on cam-size minimization.

The problem of cam-size minimization has been studied extensively in the last thirty years. This problem was first solved using graphical methods—see, e.g., (Rothbart, 1956; Hirschhorn, 1962). Since the introduction of computers in the design process, the optimization of cams was further developed by Chen (1982). The optimization of planar cams by minimizing the cam size was studied by Loeff and Soni (1975), and Mills et al. (1993), while the optimization of spatial cams was outlined by Angeles and López-Cajún (1991).

The size of the cam is usually constrained by the pressure-angle condition. Chen (1982) proved that the pressure angle can be reduced by increasing the radius of the base circle. González-Palacios and Angeles (1993) proposed a unified approach to the synthesis of cam mechanisms, and obtained the general equation for the tangent of the pressure angle for all types of cam mechanisms.

The optimization in this context becomes a nonlinear constrained problem. Chan and Kok (1996) suggested to use the Monte Carlo method to obtain the optimum parameters, whereas Bouzakis et al. (1997) suggested to use the penalty-function method to solve the nonlinear constrained problem.

The addition of an elastic torque compensator has been proven to lead to a smaller overall mechanism. Nishioka et al. (1993, 1994, and 1995) proposed the use of a cam-driven mass-spring system to compensate the input shaft torque on indexing cam mechanisms. Lam et al. (1997) proposed a synthesis methodology to the

design of a spring-cam mechanism to minimize the fluctuating torque of mechanical transmissions, the spring-cam mechanism that accomplishes this task being termed as an *elastic torque compensator* (ETC).

3. Lower-Pairs vs. Higher-Pair Mechanisms

Lower-pair mechanisms, also known as linkages, entail kinematic relations that are expressed as trigonometric equations in the sines and cosines of the angles involved -- see, e.g. (Duffy, 1980). Upon introduction of the well-known trigonometric identities relating the sine and the cosine of an angle with the tangent of half this angle, the foregoing relations become algebraic equations, i.e., multivariate polynomial equations in those tangents. As a result, the equations relating the input and output angles take the form $f(x, y) = 0$, where x and y are the tangents of half the input and the output angle, respectively. Since $f(x, y)$ is a bivariate polynomial, it is an *analytic function* of its arguments. As such, it admits only a finite, discrete set of isolated zeros -- if we disregard degenerate cases admitting a continuum of zeros. This property of linkages prevents them from producing dwell *exactly*. Indeed, dwell requiring that the output variable y remain constant during a finite interval of values of x , the relation $y = y(x)$ is necessarily *nonanalytic*, and hence, dwell cannot be produced exactly with a linkage. Approximations of dwell can be obtained with linkages by exploiting the properties of the coupler curves of four-bar linkages traced by points on special loci of the coupler link, namely, the cubic of stationary curvature and the inflection circle (Denavit and Hartenberg 1964).

Cam mechanisms, on the contrary, entail input-output equations that are of a much more general nature, and hence, accommodate nonanalytic input-output relations. This is the reason why we use cams as building blocks in this work.

CHAPTER 2

Kinematics of Cam Mechanisms and Problem Definition

A cam mechanism is a mechanical system composed of three elements: the cam; the follower; and the fixed frame. A fourth element, called the roller is usually added between the cam and the follower to improve the mechanism performance. The cam and the follower are linked by a higher kinematic pair, whereby the contact between the driving element and the driven element is either a line or a point.

Cam mechanisms are widely used in machines and instruments. Some typical examples are internal combustion engines, textile machines, machine tools, and countless automatic devices. Cam mechanisms offer important advantages, namely no-backlash; low friction; high stiffness; and virtually unlimited versatility.

1. Classification of Cam Mechanisms

Cam mechanisms are generally classified according to the type of motion they produce, the relative layout of the instant screw axes of their elements, and the follower geometry.

1.1. Type of output motion. The follower can undergo two types of motion, as illustrated in Fig. 2.1, namely,

- Translating follower: The follower is coupled to the frame by a prismatic joint.

- Oscillating follower: The follower is coupled to the frame by a revolute joint.

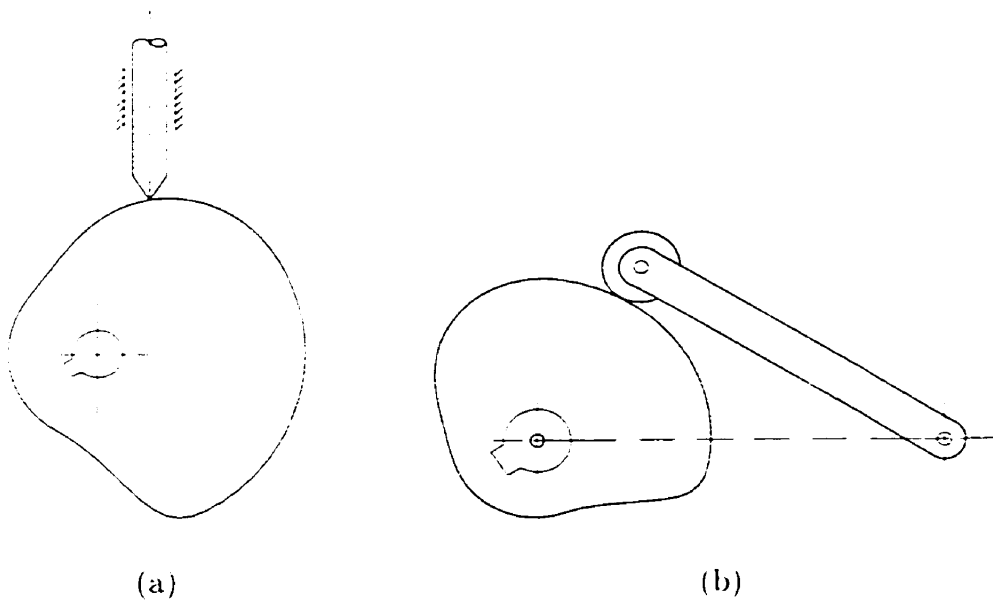


Figure 2.1: (a) Planar cam with offset knife-edge translating follower; (b) planar cam with oscillating roller-follower.

1.2. Relative layout of the instant screw axes. The instantaneous screw axis (*ISA*) is defined as the set of points with minimum velocity magnitude of two rigid-bodies undergoing relative motion (Angeles 1982). Three link cam mechanisms, i.e., the simple mechanisms consisting of cam, follower, and frame, have three *ISAs*: frame-cam; cam-follower; and follower-frame. A modified classification formulated by González-Palacios and Angeles (1991) is given below:

- Planar: Every *ISA* is either parallel to one direction for the oscillating follower, or perpendicular to it for the translating follower;
- Spherical: All *ISAs* are concurrent;
- Spatial: None of the two foregoing conditions is satisfied.

1.3. Follower configuration. The followers are classified according to their physical shape, namely:

- Knife-edge follower.

- Roller-follower.
- Flat-face follower.

Mechanisms of the first two types are those of Fig 2.1. In addition to the cam mechanisms described above, there are other types, such as conjugate cams and indexing cams. In conjugate cam mechanisms, the mechanism includes multiple cams and multiple followers. Contact takes place at multiple points, which allows for better performance and eliminates the need for springs. In indexing cam mechanisms, the follower undergoes several working cycles for one cam cycle. This is needed when similar operations or intermittent motions must be performed during each cam cycle.

2. The Displacement Program

The displacement program is a function that describes the input-output motion of the cam mechanism. The synthesis of the displacement program has been studied extensively in recent years. An overview is found in (Angeles and López-Cajún, 1991; Chen, 1982; and Koloc and Václavík, 1993). A displacement program is composed of a set of simple motions, namely, rise, return, and dwell. The functions used to describe these periods are cycloidal, polynomial, or spline functions (Angeles and López-Cajún, 1991).

3. Quick-Return Mechanisms

We decompose the quick-return mechanism into three modules, the motor, the modulating mechanism, and the *uniform-transmission stroke generator* (U-TSG), as shown in Fig. 2.2 and 2.3. Under steady-state conditions, the motor is operated at uniform speed and periodically-varying torque. The uniform speed from the motor is then modulated by the modulating mechanism to produce the required motion, as shown in Fig. 2.5, and the motion is then transmitted to the U-TSG to move the workpiece. The function of the U-TSG is to produce a uniform *velocity ratio* between the shaft of the modulating mechanism and the *tool*. Thus, the U-TSG can be a ballscrew, a belt-pulley, or a rack-and-pinion mechanism.

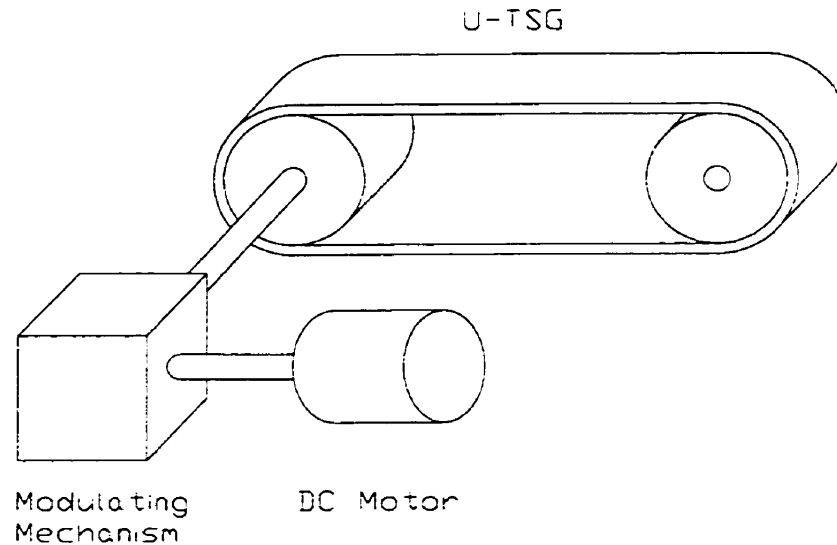


Figure 2.2: Layout of the quick-return mechanism

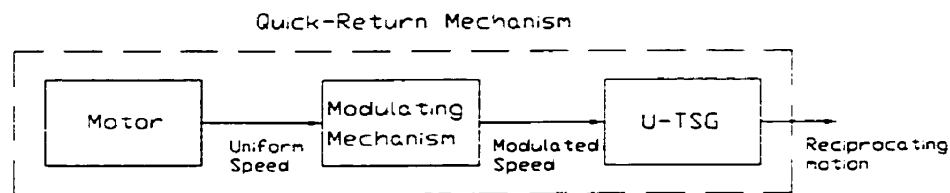


Figure 2.3: Module of the quick-return mechanism

There are three possible relative layouts of the axis of the motor and the axis of the U-TSG, as shown in Fig. 2.4, i.e.,

- co-axial;
- parallel;
- intersecting.

The modulating mechanism can be subdivided into submodules, the function of each submodule being explained in Table 2.1. The purpose of the reducer is to step down the high velocity from the motor such that a cycle of the primary cam is equal to the period required for each operation. A speed reducer based on cam mechanisms, Speed-o-Cam (González-Palacios and Angeles, 1998), is selected to accomplish this task. Since the reducer is a mechanism based on cams, it has the advantage of

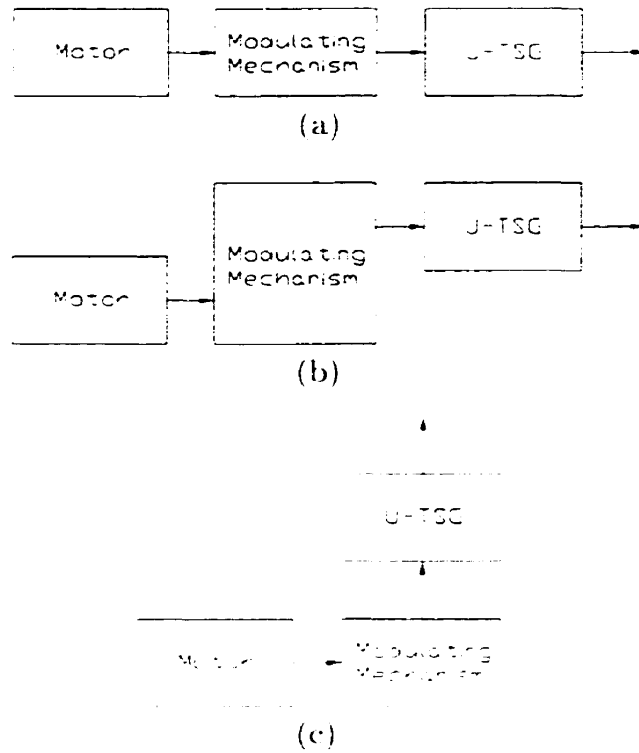


Figure 2.4: Relative layouts of the axes of the motor and the U-TSG: (a) co-axial, (b) parallel, and (c) intersecting

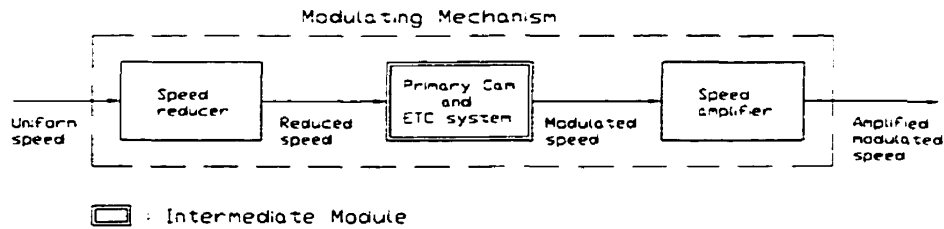


Figure 2.5: Modules of the modulating mechanism

low friction, no backlash, and high stiffness, as compared to gears. The task of the primary cam mechanism is to modulate the uniform motion of the motor to produce the required motion for the task. The motion of the follower is then amplified using a speed amplifier, Speed-o-Cam again, to produce the required quick-return motion.

Table 2.1: Cam elements of the quick-return mechanism

Intermediate Module	Function
Primary cam mechanism	Modulates the uniform speed and velocity from the input shaft of the motor:
Elastic torque compensator	Eliminates the required torque fluctuations from the motor.

Table 2.2: Characteristics of the U-TSG

Belt-Pulley	<ul style="list-style-type: none"> • The axis of the input shaft is perpendicular to the direction of motion of the tool. • The characteristic length of the tool actuator is defined by the radius of the pulley. • Flexibility added to the overall system. • Low-Cost, can be easily customized to any size.
Ball screws	<ul style="list-style-type: none"> • The axis of the input shaft of the ball-screw is parallel to the direction of motion of the tool. • The characteristic length of the tool actuator is defined as the pitch of the screw. • Constrained by the size and pitches available commercially.
Rack-and-Pinion	<ul style="list-style-type: none"> • The axis of the input shaft of the rack-and-pinion is perpendicular to the direction of motion of the tool. • The characteristic length of the tool actuator is defined by the radius of the pitch circle of the pinion. • Constrained by the racks-and-pinions available commercially.

4. Long-Stroke, Quick-Return Mechanisms

The method proposed in this thesis is applied to the design of long-stroke, quick-return mechanisms. Three types of U-TSG can be used, these are the belt-pulley, ball-screw, and rack-and-pinion mechanisms, as summarized in Table 2.2.

A long-stroke mechanism is understood in this context as one whose stroke length is at least one order of magnitude greater than the *characteristic length* of the U-TSG, as defined in Table 2.2. The layout of the quick-return mechanism, in block form, is shown in Fig. 2.6, where ω denotes the angular speed of the motor rotor; $\dot{\alpha}$ the reduced speed, which is the speed of the cam; $\dot{\phi}$ the *modulated* speed of the follower;

$\dot{\theta}$ the amplified speed of the follower; \dot{s} the translational speed of the tool or the workpiece. The input-output relationships of the building elements are given below:

$$\begin{aligned}\dot{s} &= N_{\text{act}} \dot{\theta} \\ \dot{\theta} &= N_{\text{amp}} \dot{\phi} \\ \dot{\phi} &= \dot{\phi}(\psi) \dot{\psi} \\ \dot{\psi} &= N_{\text{red}} \omega\end{aligned}$$

For belt-pulley systems $N_{\text{act}} = \pi r$ (m/rad), where r is the radius of the belt-pulley; for ball screws $N_{\text{act}} = 2\pi p$ (m/rad), where p is the pitch of the screw; for rack-and-pinions, $N_{\text{act}} = \pi r$ (m/rad), where r is the radius of the pitch circle of the pinion.

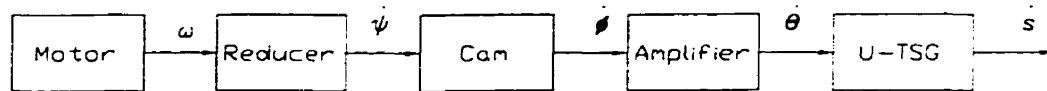


Figure 2.6: Layout of the quick-return mechanism

5. Problem Definition

This thesis focuses on the optimization of quick-return mechanisms by optimizing its cam mechanisms. An important aspect of cam design is the minimization of cam mass. A compact design has a small volume and, hence, small mass. The mass of the cam affects the dynamic properties of the transmission, which comprises items such as inertia forces. In addition to the material cost, a cam with large volume needs a large motor, thus further increasing the cost and volume of the overall mechanism. By demodulating the required torque, such that the motor is always operating at its nominal speed, the size of the motor can be further reduced.

The aim is to develop two methodologies. One is to optimize cam mechanisms by minimizing their size. The second is to propose a methodology for the design of an elastic torque-compensation mechanism to demodulate the required torque.

CHAPTER 3

Cam-Size Minimization Under Pressure-Angle Bounds

Cam-size minimization is understood here as the process of selecting the geometric parameters of a cam-follower mechanism of the smallest possible size, while observing constraints on performance indicators such as pressure angle, cam-profile radius of curvature, etc. The approach presented in this chapter is a streamlined version of the method proposed by Angeles and López-Cajún (1991). The objective is to develop a unified method for the optimization of cam mechanisms.

1. Pressure Angle

The main task of a mechanism is to transmit motion and force. The most widely used factor to describe the force-transmission characteristics of cam mechanisms is the pressure angle, α , as depicted in Fig. 3.1. This concept is defined as the angle between the force exerted by the cam on the follower and the velocity of the contact point on the follower. Ideally, the pressure angle should be zero, but, as the cam rotates, the pressure angle α varies as a function of the angle ψ of rotation of the cam. Therefore, the pressure angle is usually bounded between two values, $\pm \alpha_M$. A value of α_M that is widely accepted is 30° (Rothbart 1956).

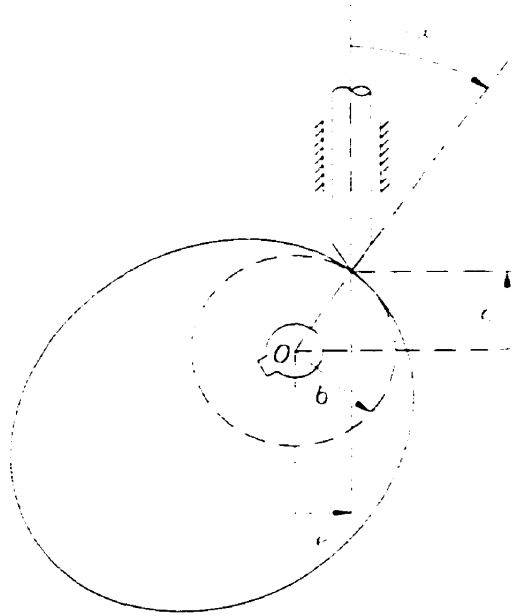


Figure 3.1: Pressure angle of the translating follower

2. Determination of the Occurrence of the Maximum Pressure Angle

For any type of cam, either planar, cylindrical, spherical, or spatial, the tangent of the pressure angle can be expressed in the form

$$\tan \alpha = \frac{N(\psi)}{D(\psi)} \quad (3.1)$$

where, α , N , and D are functions of the angle ψ . The tangent of the pressure angle for the general type of cam mechanisms was obtained by González-Palacios and Angeles (1993).

The maximum pressure angle occurs when the first derivative of the pressure angle with respect to ψ vanishes. The optimization problem becomes one of finding the values of ψ that make $|\alpha|$ a maximum. To this end, the *extrema* of $\tan \alpha$ are first found, which is done by taking the derivative of both sides of eq.(3.1) with respect to ψ , and setting this derivative equal to zero, i.e.,

$$\frac{d \tan \alpha}{d \psi} = 0 \quad (3.2)$$

which gives, successively,

$$\alpha'(\psi) \sec^2 \alpha = \frac{1}{D} [N' - (\tan \alpha) D'] \quad (3.3a)$$

$$F(\psi) \equiv N'(\psi) - \tan \alpha(\psi) D'(\psi) = 0 \quad (3.3b)$$

which is verified at values $\psi = \psi^*$, where $|\alpha|$ attains its maximum α_M .

Equation (3.3b) then becomes the *extremality condition* for the pressure angle. Additional constraints, if needed, are obtained from the cam geometry, thus finally obtaining a function $F = F(\psi^*)$, from which ψ^* is to be found. The problem thus reduces, in some instances, to solving a nonlinear equation of only one variable, namely, $F(\psi^*) = 0$, which can be readily accomplished using any graphical or numerical methods.

3. Translating Follower

The study of the knife-edge translating follower is equivalent to the study of the roller translating follower. They both have the same pressure angle distribution, where the profile of the cam with the knife-edge follower being described by the trajectory of the centre of the follower-roller.

The follower-displacement program of a cam mechanism is usually given as the sum of a constant and a positive-semidefinite function $\sigma(\psi)$. For a cam with translating follower, the constant is c , which represents the smallest displacement of the follower, Fig. 3.2. The displacement of the follower can be written as

$$s(\psi) = c + \sigma(\psi) \quad (3.4a)$$

A plot of $F(\psi)$ is displayed in Fig. 3.3, which shows that this function vanishes both during dwell and at an isolated value within the rise and the return phases. We are obviously interested in finding these isolated values. Therefore, there are only two sets of solutions. Either the pressure angle reaches a maximum during the rise phase and a minimum during the return phase, or reaches a minimum during the rise phase and a maximum during the return phase.

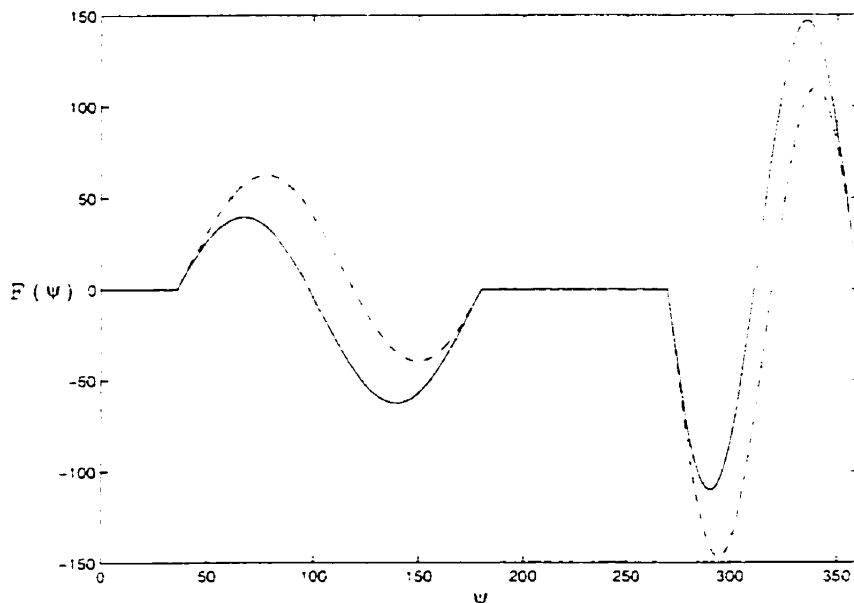


Figure 3.3: Plot of the function defining the extremality condition of a translating quick-return cam mechanism. The dashed plot corresponds when $\alpha = \alpha_M$

From eq. (3.6), we have the following relationship at the extrema:

$$\pm c \tan \alpha_M + e = \sigma'^* \mp \sigma^* \tan \alpha_M \quad (3.8)$$

Let σ_1^* and σ_2^* be the value of σ^* when the pressure angle reaches a maximum and a minimum, respectively. Therefore,

$$c \tan \alpha_M + e = \sigma_1'^* - \sigma_1^* \tan \alpha_M \quad (3.9a)$$

$$-c \tan \alpha_M + e = \sigma_2'^* + \sigma_2^* \tan \alpha_M \quad (3.9b)$$

Solving for the parameters c and e from eqs.(3.9a & b) gives

$$c = \frac{\sigma_1'^* - \sigma_1^* \tan \alpha_M - \sigma_2'^* - \sigma_2^* \tan \alpha_M}{2 \tan \alpha_M} \quad (3.10a)$$

$$e = \frac{\sigma_1'^* - \sigma_1^* \tan \alpha_M + \sigma_2'^* - \sigma_2^* \tan \alpha_M}{2} \quad (3.10b)$$

Finally, from the geometry of the translating cam mechanism, the radius of the base circle of the optimum cam is

$$b = \sqrt{e^2 + c^2} \quad (3.11)$$

4. Oscillating Follower

The pressure angle of the oscillating follower is derived in (Angeles and López-Cajún, 1991) as

$$\tan \alpha = \frac{u[1 + \phi'(\psi)] - \cos \phi}{\sin \phi} \quad (3.12)$$

where ϕ is the angular displacement of the follower, ϕ' is the derivative of ϕ with respect to ψ , and u is the length of the follower arm e divided by the distance l between the axes of rotation of the cam and of the follower, as shown in Fig. 3.4.

The *extremality condition* of eq.(3.3b) now takes the form

$$u\phi''(\psi) + \phi'(\psi) \sin \phi = \pm \tan \alpha_M \phi'(\psi) \cos \phi \quad (3.13)$$

which is verified at values $\psi = \psi^*$ at which $|\alpha|$ attains its maximum α_M .

The follower-displacement program can be given as the sum of a constant β and a positive-semidefinite function $\sigma(\psi)$, where β is the value of ϕ at the lowest position of the follower. The angular displacement of the follower is then,

$$\phi(\psi) = \beta + \sigma(\psi) \quad (3.14a)$$

equations in four unknowns, u , β , σ_1^* , and σ_2^* , namely

$$u\sigma_1''^* + \sigma_1'^* \sin(\beta + \sigma_1^*) - \tan \alpha_M \sigma_1'^* \cos(\beta + \sigma_1^*) = 0 \quad (3.17a)$$

$$u\sigma_2''^* + \sigma_2'^* \sin(\beta + \sigma_2^*) + \tan \alpha_M \sigma_2'^* \cos(\beta + \sigma_2^*) = 0 \quad (3.17b)$$

$$u[1 + \sigma_1'^*] - \cos(\beta + \sigma_1^*) - \sin(\beta + \sigma_1^*) \tan \alpha_M = 0 \quad (3.17c)$$

$$u[1 + \sigma_2'^*] - \cos(\beta + \sigma_2^*) + \sin(\beta + \sigma_2^*) \tan \alpha_M = 0 \quad (3.17d)$$

The four unknowns of the foregoing problem can be determined using the Newton-Raphson method.

5. Graphical User Interface

The method proposed in the previous sections is implemented in the MATLAB environment. In addition, a graphical user interface (GUI) is built using the MATLAB interactive GUI Builder to aid the designer during the design process.

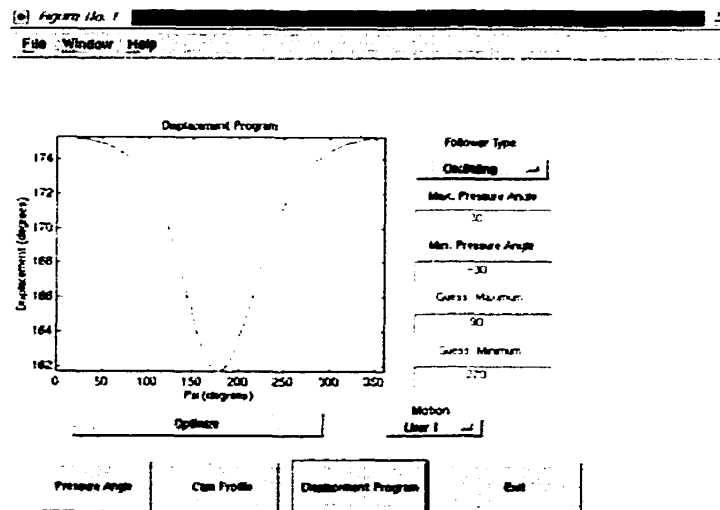


Figure 3.5: Graphical user interface

The interface consists of the main display area, the input areas, pull-down menus, and the push buttons, as shown in Fig. 3.5. Their functions are explained in Table 3.1.

Follower type	:	Select the type of follower
Max. Pressure Angle	:	set the maximum allowed pressure angle
Min. Pressure Angle	:	set the minimum allowed pressure angle
Guess Maximum	:	initial guess of the location of the maximum pressure angle
Guess Minimum	:	initial guess of the location of the minimum pressure angle
Motion	:	select the displacement program
Optimize	:	obtain the optimum cam parameters
Pressure Angle	:	display the pressure angle distribution
Cam Profile	:	display the cam profile
Displacement Program	:	display the displacement program
Exit	:	exit the program

Table 3.1: GUI functions

There are two pull-down menus. The user can select the type of the follower, either translating follower or oscillating follower, with the *Follower Type* pull-down menu. The user can also select the type of motion with the *Motion* pull-down menu.

After providing the type of follower, the displacement program, the maximum and minimum pressure angles, and the initial guesses, the user must press *Optimize*, the program will then calculate the optimum values of the cam parameters. The user can display the cam profile and the pressure angle distribution in the main display area.

Since the method is iterative, the user may have to try with several initial conditions to arrive to a cam mechanism with minimum size. If no initial guess is provided, the default value is the midpoint of the rise and the return phases.

CHAPTER 4

Optimization of the Elastic Torque Compensator

The objective of this chapter is to develop a methodology to design and synthesize a cam-spring mechanism to compensate the load variations due to a periodic torque. Motors are most efficient when they operate under constant velocity and torque. For the case of a cam-follower system, the required velocity is usually constant, but the required torque is periodic, because the velocity of the follower fluctuates periodically. The solution is to use a cam-spring mechanism to compensate the fluctuating torque (Nishioka et al. 1993, 1994a, 1994b, and 1995). The main purpose of the spring is to absorb energy from the system when the required torque is low, and release energy to the system when the required torque is high. Using this mechanism, depicted in Fig. 4.1, the motor can be operated at constant velocity. The cam-spring system was termed an *elastic torque compensator* (ETC) in (Lam et al., 1997).

1. Nomenclature

The notation used to describe the cam-spring system is listed below:

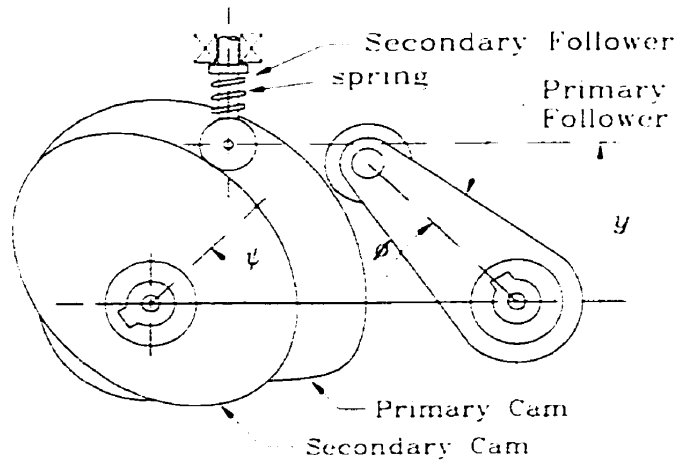


Figure 4.1: The overall ETC system

- y : displacement of the translating follower of the cam-spring system.
 y_0 : value of y when the spring is uncompressed.
 I_c : moment of inertia of the cam.
 I_f : moment of inertia of the follower.
 k : spring constant.
 \dot{z} : first derivative of the arbitrary variable z with respect to time.
 z' : first derivative of the arbitrary variable z with respect to t .

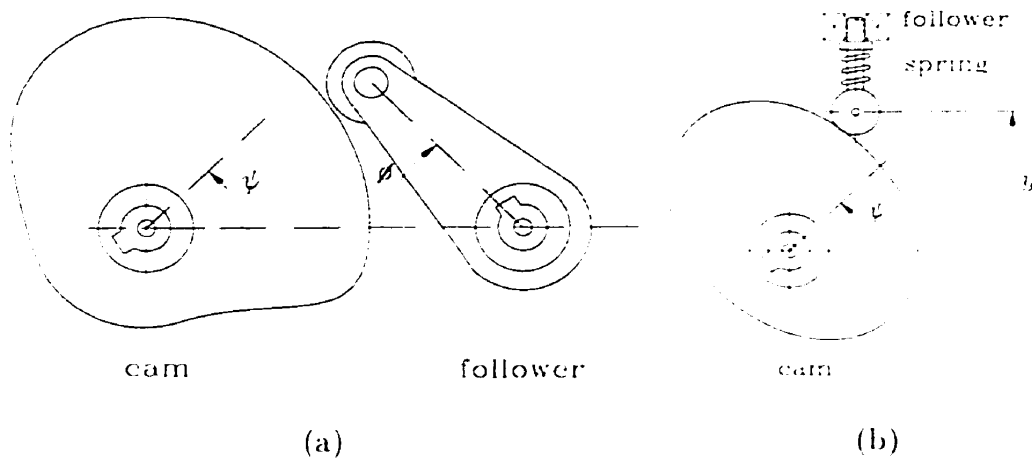


Figure 4.2: Layout of (a) the primary system and (b) the ETC system

2. Mechanism Dynamics and Mathematical Model

The mathematical model of the mechanism is derived using the Lagrangian formulation:

$$\frac{\partial}{\partial t} \left(\frac{\partial L}{\partial \dot{c}} \right) - \frac{\partial L}{\partial c} = f \quad (4.1)$$

where L is the Lagrangian, and f is the generalized force.

The kinetic and potential energies are represented by T and V , respectively. It is assumed that the potential energy consists of only the elastic energy stored in the spring, and hence,

$$\begin{aligned} L &\equiv T - V \\ T &= \frac{1}{2} I_c \dot{c}^2 + \frac{1}{2} I_f \dot{\phi}^2 = \frac{1}{2} I_c \dot{c}^2 + \frac{1}{2} I_f (\phi'(c))^2 \dot{c}^2 \\ V &= \frac{1}{2} k [y(c) - y_0]^2 \end{aligned} \quad (4.2)$$

Therefore, the first and second terms of the Lagrange equation (4.1) become

$$\frac{\partial}{\partial t} \left(\frac{\partial L}{\partial \dot{c}} \right) = I_c \ddot{c} + I_f (\phi'(c))^2 \ddot{c} + 2I_f \phi'(c) \phi''(c) \dot{c}^2 \quad (4.3)$$

$$\frac{\partial L}{\partial c} = I_f \phi'(c) \phi''(c) \dot{c}^2 - k [y(c) - y_0] y'(c) \quad (4.4)$$

Substituting eqs.(4.3a & b) into eq.(4.1) gives the mathematical model

$$[I_c + I_f (\phi'(c))^2] \ddot{c} + I_f \phi'(c) \phi''(c) \dot{c}^2 + k [y(c) - y_0] y'(c) = \tau(c) \quad (4.5)$$

where $\tau(c)$ is the motor supplied torque. Under steady-state conditions, $\ddot{c} = 0$, and $\dot{c} = \omega_o = \text{constant}$, the latter being the operating speed. In addition, the torque required vanishes since power losses are neglected in this model. The mathematical model that describes the steady-state regime is,

$$I_f \phi'(c) \phi''(c) \omega_o^2 + k [y(c) - y_0] y'(c) = 0 \quad (4.6)$$

Equation (4.6) admits the integral

$$I_f(\phi'(\psi))^2\omega_o^2 + k[y(\psi) - y_0]^2 = A \quad (4.7)$$

where A is an integration constant. Note that the value of A represents two times the sum of the value of the kinetic energy stored in the mechanism and the potential energy stored in the spring.

For continuity, the value of $y(\psi) - y_0$ must have a constant sign, but zero values are also admissible. If we assume that $y(\psi) - y_0$ is nonnegative, then

$$y(\psi) - y_0 \geq 0 \quad (4.8)$$

For an optimum design, the spring should be uncompressed at the lowest follower position. However, in practice it is advantageous to preload the spring in order to maintain contact between the cam and the follower at all times. For the ideal case when there is no separation between the cam and the follower, let

$$\begin{aligned} \min_{\psi} \{y(\psi) - y_0\} &= 0 \\ \max_{\psi} \{|\phi'(\psi)|\} &= \phi'_M \end{aligned} \quad (4.9)$$

Hence, eq.(4.7) yields

$$I_f\phi'_M{}^2\omega_o^2 = A \quad (4.10)$$

Moreover, when $\phi'(\psi) = 0$, we want

$$k[y(\psi) - y_0]^2 = A$$

or

$$\max_{\psi} \{k[y(\psi) - y_0]^2\} = A \quad (4.11)$$

Let

$$h = \max_c \{y(c) - y_0\} \quad (4.12)$$

Substituting eq.(4.10) into eq.(4.11) yields

$$kh^2 = I_f \phi_M'^2 \omega_o^2 \quad (4.13a)$$

or

$$k = I_f \frac{\phi_M'^2}{h^2} \omega_o^2 \quad (4.13b)$$

Since the size of the secondary cam increases with respect to the maximum distance travelled by the follower, h , we should aim at minimizing the value of h or at maximizing the value of k .

After the appropriate spring constant is selected, the cam profile of the secondary system can be calculated with the follower-displacement program derived from eq.(4.7), namely,

$$y(c) = \omega_o \sqrt{\frac{I_f(\phi_M'^2 - \phi'^2(c))}{k}} \quad (4.14)$$

3. Selection of the Spring Constant

The spring is designed such that the natural frequency of the spring-follower system avoids resonance with the reciprocating input motion $\phi(c)$. In addition, the spring is designed for minimum spring material.

3.1. Lower Bound. In high-speed cam applications, such as in aircraft or in automobile engines, a rapid reciprocating motion of the follower is usually produced. In these cases, it is important to avoid resonance between the reciprocating motion of the end of the spring and the natural frequencies of vibration of the spring-follower system.

For a cam mechanism with an input angular velocity of ω_o (rad/s), the position of the spring is given as a function of time in the form

$$y(t) = \sigma(\omega_o t) \quad (4.15)$$

where ω_o is in terms of the input angle, and it describes the input-output relationship of the mechanism.

The displacement function $y(t)$ produced by the cam can be quite complicated, it is usually nonanalytic, but in any event, it is periodic. Hence, this function can be approximated by a Fourier series (Kreyszig 1988), namely,

$$y(t) = a_0 + \sum_{n=1}^{\infty} (a_n \cos n\omega_o t + b_n \sin \omega_o t) \quad (4.16)$$

where

$$\begin{aligned} a_0 &= \frac{\omega}{2\pi} \int_0^{2\pi/\omega} f(t) dt \\ a_n &= \frac{\omega}{\pi} \int_0^{2\pi/\omega} f(t) \cos(n\omega_o t) dt \quad n = 1, 2, \dots \\ b_n &= \frac{\omega}{\pi} \int_0^{2\pi/\omega} f(t) \sin(n\omega_o t) dt \quad n = 1, 2, \dots \end{aligned}$$

In general, amplitudes of the higher harmonics decrease as the order of the harmonic increases. For the case of engine valves, the highest significant Fourier component is roughly the thirteenth harmonic (Wahl 1944).

To calculate the error of the approximation, we use Parseval's theorem, (Kreyszig 1988). The theorem states that the root-mean square value of the periodic function at hand equals the square root of the sum of the squares of the Fourier coefficients, with the first one being taken twice, i.e.,

$$\frac{\omega}{\pi} \int_0^{2\pi/\omega} y(t)^2 dt = 2a_0^2 + \sum_{n=1}^{\infty} (a_n^2 + b_n^2) \quad (4.17a)$$

If the periodic function is approximated to the N th harmonics, the least square error of the approximation, e , can be found using eq.(4.17b). Note that the sum of square

of real numbers on the right side of eq.(4.17b) cannot be negative. Hence, with increasing N , the least square error decreases.

$$e = \int_0^{\frac{2\pi}{\omega}} y(t)^2 dt - \frac{\pi}{\omega} \left[2a_0^2 + \sum_{n=1}^N (a_n^2 + b_n^2) \right] > 0 \quad (4.17b)$$

An error of about 0.1% usually accepted.

To avoid resonance, the spring should be stiff enough so that the lowest natural frequency of the system is considerably higher than the highest significant harmonic of the output motion of the follower. If the damping and the mass of the spring are neglected, the mathematical model of the spring-follower system can be written as.

$$m \frac{d^2 y}{dt^2} + ky = 0 \quad (4.18)$$

where the natural frequency of the system is.

$$\omega_n = \sqrt{\frac{k}{m}}$$

or

$$k = m\omega_n^2 \quad (4.19a)$$

Rearranging eq.(4.13a), we obtain

$$h = \sqrt{\frac{I_f \phi_M^2 \omega_o^2}{k}} \quad (4.19b)$$

3.2. Optimum Design of Helical Springs. As shown in the previous sections, it is advantageous to select a high spring constant. However, if the spring constant is large, the force acting on the cam is also large, thus resulting in undesirable forces on the bearings and increasing wear. Therefore, at the most compressed condition of the spring, the torsional shear stress must not exceed a specified value τ_d . If only the torsional shear stress and active coils are considered, Spotts (1985) showed

that if the spring is designed so that the minimum load (P_{min}), stress (τ_{min}), and deflection are exactly one-half the maximum load (P_{max}), stress (τ_{max}) and deflection, the spring will contain the least possible amount of material.

The value of τ_{max} is selected according to the material of the spring. A set of curves describing material properties with recommended design stresses can be found in (Carlson, 1978). For the optimum spring,

$$\tau_{min} = \frac{\tau_{max}}{2}; \quad P_{min} = \frac{P_{max}}{2} \quad (4.20)$$

Assuming that the major stress in the spring is torsional shearing stress and selecting a mean coil radius R , the other spring parameters are obtained from eqs(4.21a b) as

$$d = \left(\frac{16P_{max}R}{\pi\tau_{max}} \right)^{1/3} \quad (4.21a)$$

$$N = \frac{d^4 Gh}{64(P_{max} - P_{min})R^3} \quad (4.21b)$$

where

d : diameter of the wire;

R : mean coil radius, the average of the inside and outside radii;

N : number of coils;

G : modulus of elasticity, shear stress;

P : load;

CHAPTER 5

Applications

1. Design of a Long-Stroke Quick-Return Mechanism

The case under study arises in the production of veneer. A quick-return mechanism is needed to transport and glue veneer strips with the dimensions of 3 m length, 0.30 m width, and 8 mm of thickness. The stroke of the mechanism is 3 m and the period required for each operation is about 2 s. The quick-return motion is described in Table 5.1, and illustrated in Figures 5.1 and 5.2. The forward and return motions are approximated using a 4-5-6-7 polynomial such that the displacement, velocity, acceleration, and jerk are smooth at the end points.

The long-stroke motion can be implemented by means of a slider driven either by the belt of a belt-pulley mechanism or by the nut of a ball screw. We discuss the two cases below.

Motion	Period(%)
Dwell	20
Forward Phase	40
Dwell	20
Return Phase	20

Table 5.1: Quick-return motion

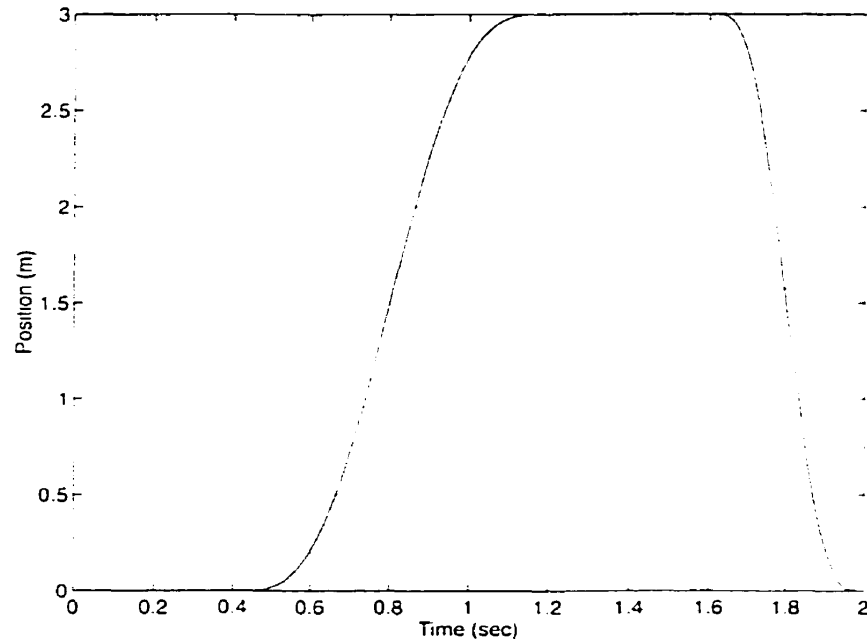


Figure 5.1: Quick-return motion

c/l	β (deg)	b/l
0.585	47.75	0.7453

Table 5.2: Parameters of the cam for the belt-pulley mechanism

1.1. Belt-Pulley mechanism. We use a pulley made of aluminium with a diameter of $D_p = 0.1$ m and thickness of $t_p = 0.012$ m. The speed amplifier is selected with a ratio of 1 : 16.

Therefore the oscillating follower must make a maximum sweep of

$$\phi = \frac{l}{\pi D_p \cdot N_{amp}} = \frac{3}{\pi(0.1)(16)} = 0.5968 \text{ rad} = 34.2^\circ$$

Using a DC motor operating at its nominal speed of 3000 rpm, with a speed reducer with ratio of 100 : 1, each operation takes exactly 2 seconds to perform.

Applying the method developed in the previous chapters, the optimum parameters of the cam are obtained and shown in Table 5.2. The pressure angle distribution and the profile of the cam for the belt-pulley mechanism are shown in Fig. 5.3 and 5.4.

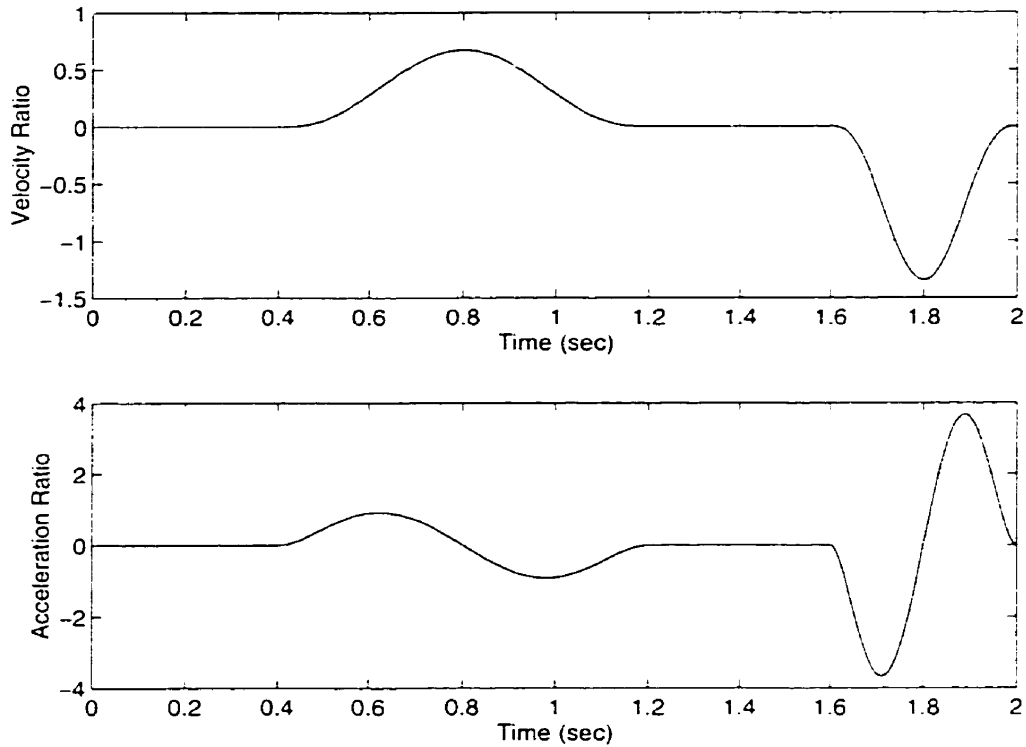


Figure 5.2: Velocity and acceleration of the quick-return motion

1.1.1. *Design of the roller.* In order to avoid undercutting and large contact stresses between the cam and the roller, the radius of the roller must be as high as possible. We choose this radius here as a fraction of the minimum radius of curvature of the pitch curve. Note that a bigger roller radius would produce undercutting. The procedure to design the roller for cam mechanisms is shown in Appendix A. Using a design factor of 2, the maximum radius of the roller is set to be 50% of the minimum radius of curvature. From Fig. 5.5, the maximum curvature is 38.8790 m^{-1} . With the design factor taken into consideration, the normalized radius of the roller is found to be $a/\ell = 0.1608$.

To compare with the results obtained by Asselin and Doléac (1997), the value of ℓ is set to be 0.08 m and the values of the other cam parameters are shown in Table 5.3.

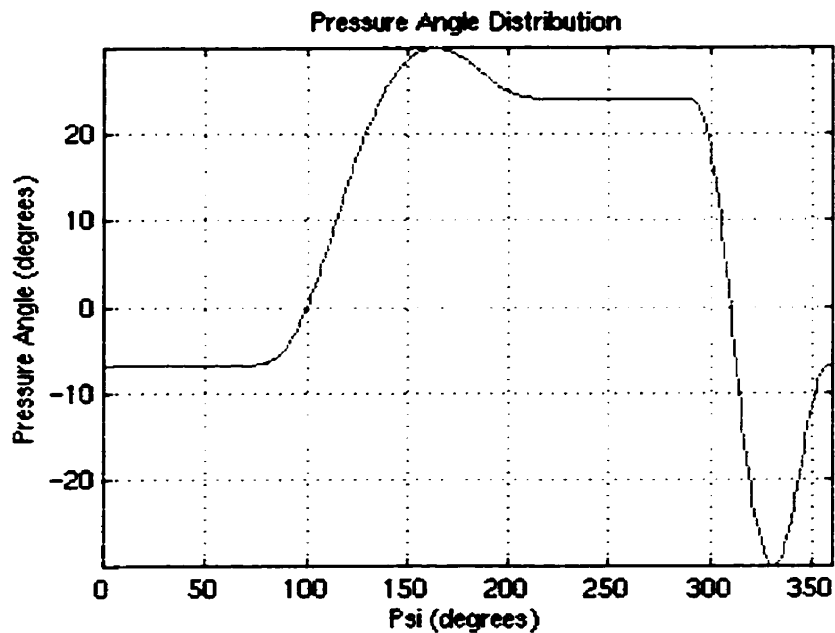


Figure 5.3: Pressure angle distribution for a belt-pulley mechanism

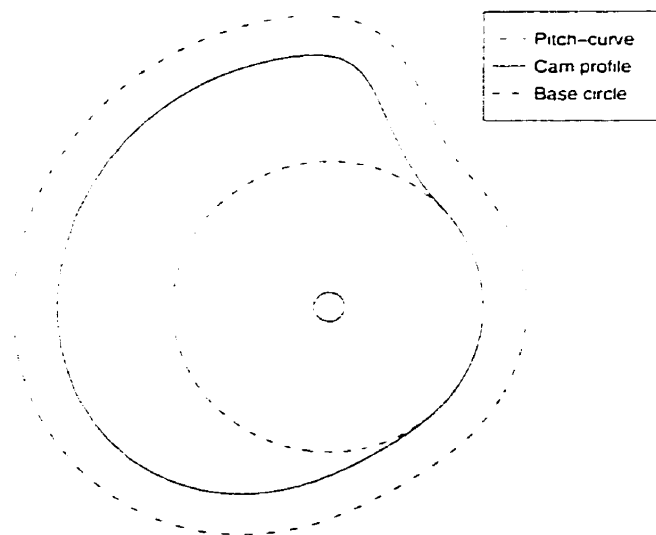


Figure 5.4: Profile of the minimum-size cam for the belt-pulley mechanism

1.1.2. *Equivalent moment of inertia.* The equivalent moment of inertia is that induced by all the moving parts linked to the follower. These include the inertia of the follower link, of the amplifier, and of all the moving parts of the belt-pulley

5.1 DESIGN OF A LONG-STROKE QUICK-RETURN MECHANISM

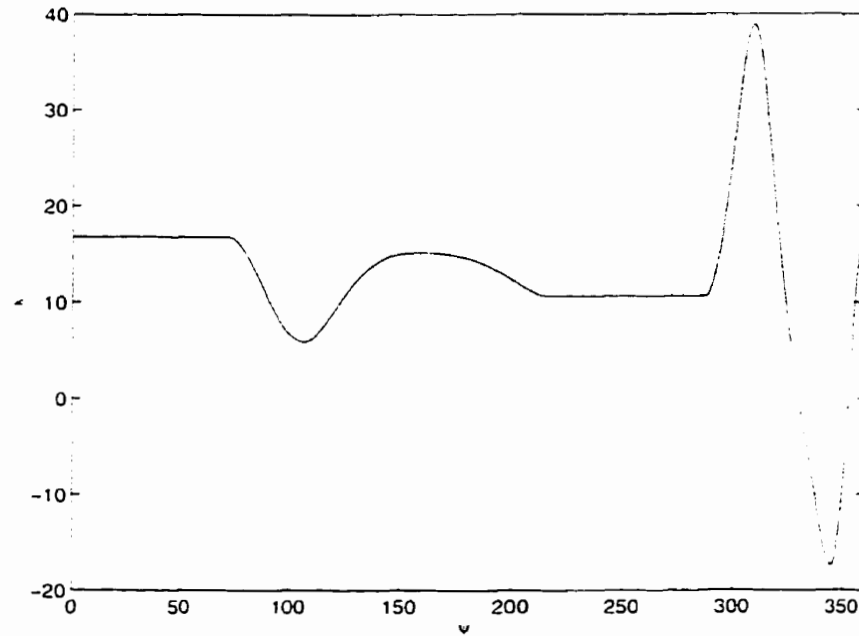


Figure 5.5: Plot of the curvature

e	0.0468 m
l	0.0800 m
b	0.0596 m
a	0.0129 m
β	47.75°

Table 5.3: Parameters of the cam

mechanism. Because of the amplification, the equivalent inertia due to the follower and the inertia of the amplifier are several orders of magnitude smaller than the inertia due to the belt-pulley mechanism. Therefore, the inertia of the follower and amplifier are ignored. For a mechanism with two pulleys, the equivalent inertia is

$$I_f = (2I_s + I_o) \cdot N_{amp}^2 \quad (5.1)$$

where

5.1 DESIGN OF A LONG-STROKE QUICK-RETURN MECHANISM

I_f : equivalent moment of inertia of the follower:

I_s : moment of inertia of one pulley:

I_o : moment of inertia due to the mass of the transported object, and fixtures.

It was estimated that the mass of the transported object is 0.72 kg, and the mass of the fixtures is 0.4 kg. For the elements in translation,

$$I_o = m_o \frac{D_p^2}{4} = 1.12 \times 10^{-4} \text{ kg m}^2$$

For a pulley made of aluminium with density of $\rho = 2.71 \times 10^3 \text{ kg/m}^3$,

$$I_s = \frac{\pi}{16} \rho D_p^4 t_p = 6.385 \times 10^{-4} \text{ kg m}^2$$

Then,

$$I_f = (0.001277 + 1.12 \times 10^{-4}) \times 16^2 = 0.3556 \text{ kg m}^2$$

The fluctuating portion of the torque on the axis of the follower is shown in Fig. 5.6. Since there is a large torque fluctuation, the addition of an ETC is needed to reduce the load on the motor.

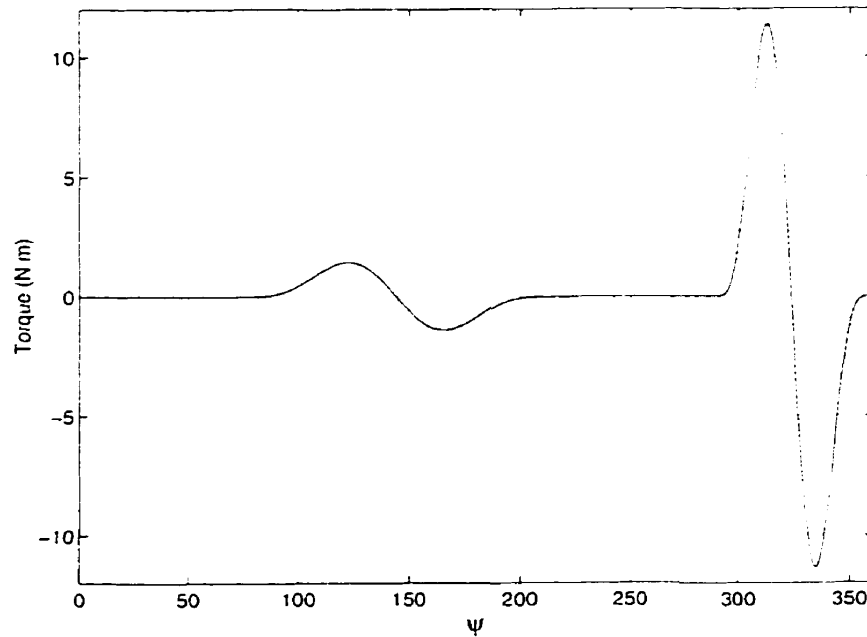


Figure 5.6: Fluctuating torque on the axis of the follower

1.1.3. *Design of the ETC.* The displacement program is approximated using the Fourier series to find the highest significant harmonic. The spectrum of the Fourier coefficients is shown in Fig. 5.7. From this figure it is apparent that the magnitude of the coefficients decreases as their order increases. If the function is approximated to the 5th harmonic, the error of the approximation is about 0.0922%. To avoid resonance, the natural frequency of the spring-follower system is set to be

$$\omega_n = 5\omega_o$$

where ω_o is the nominal speed of the DC motor.

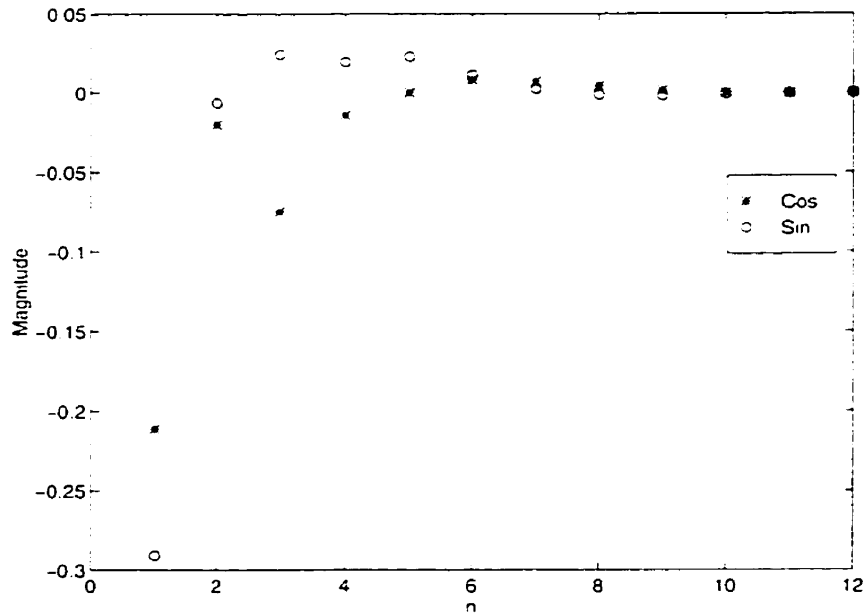


Figure 5.7: Spectrum of the Fourier coefficients

Assuming that the translating follower of the ETC has a mass of 0.1 kg, the optimum spring constant is found to be $k_{opt} = 2467$ N/m, while, from the displacement program, $\phi'_{max} = 1.3459$. Therefore, from eq.(4.19b),

$$h_{opt} = \sqrt{\frac{I_f \phi'_{max}{}^2 \omega_o^2}{k}} = 0.0499\text{m}$$

	Optimum spring	Suboptimum spring
h	0.0586 m	0.0761 m
c	0.1744 m	0.1146 m
b	0.1744 m	0.1146 m
e	0	0
a	0.0131 m	0.0114 m

Table 5.4: Parameters of the ETC cam

The optimum displacement program of the ETC is shown in Fig. 5.8a. It should be noted that the displacement program is not smooth during the full cycle. If the

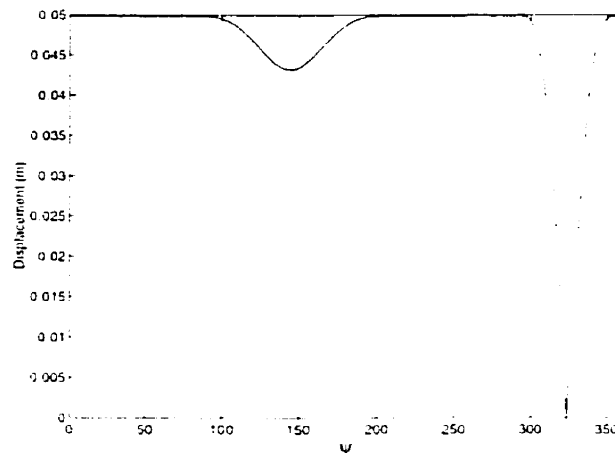


Figure 5.8: Displacement of the spring for the optimum displacement program

ETC system is designed such that the spring is optimum, the maximum displacement of the spring must be increased to the point where the minimum displacement is one half of the maximum value, as shown in Fig. 5.9a. But as Table 5.4 shows, the cam size for the mechanism with the optimum spring is quite large. The value of the maximum displacement is selected to be $h = 0.0761$ m, as shown in Fig. 5.9b, such the cam size of the ETC system is similar to the size of the primary cam.

The parameters for the cam of the ETC are given in Table 5.4. The cam profile, the pitch-curve, and the base circle are shown in Fig. 5.10.

5.1 DESIGN OF A LONG-STROKE QUICK-RETURN MECHANISM

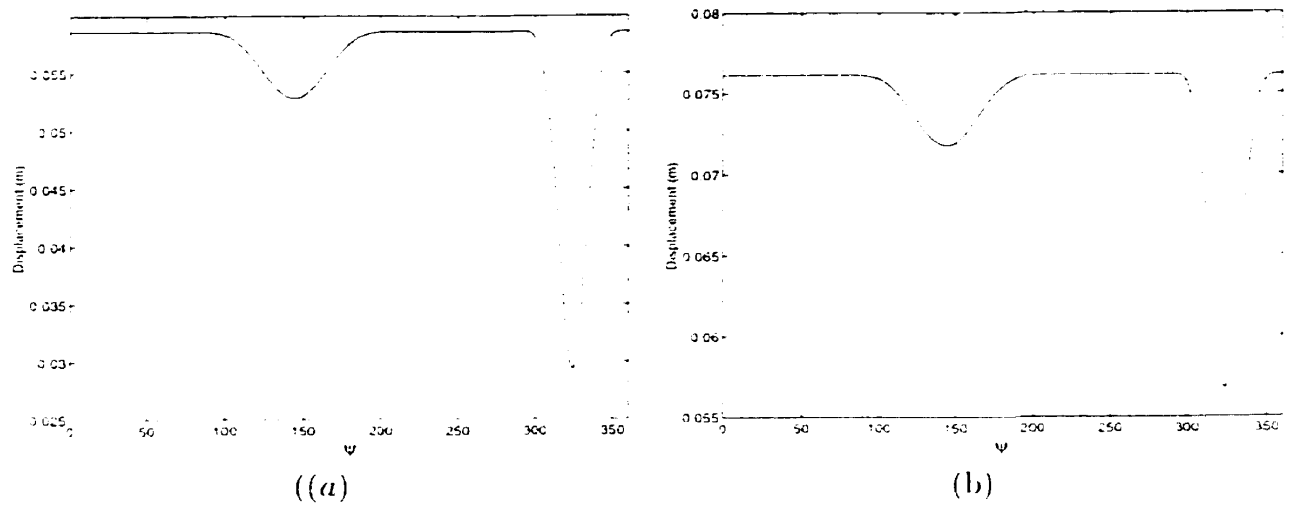


Figure 5.9: Displacement of the spring: (a) optimum spring: (b) suboptimum spring

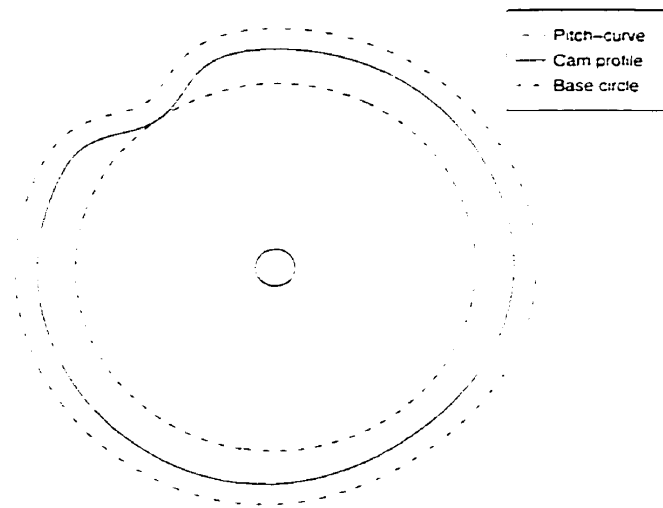
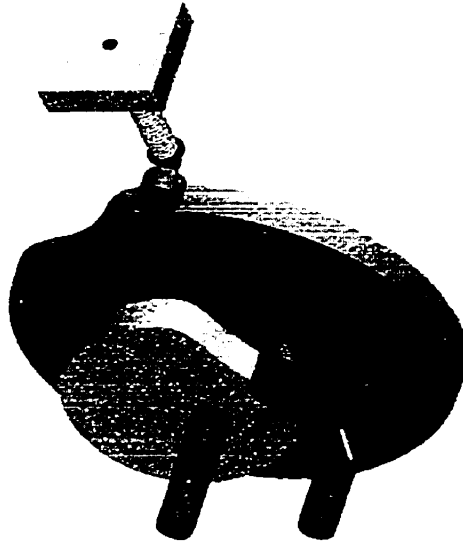


Figure 5.10: Cam profile of the ETC

Using stainless steel wire with design torsional shear stress of $\tau_d = 750$ MPa, and modulus of elasticity of $G = 69$ GPa, the parameters of the optimum spring are shown in Table 5.5.

The 3-D model of the modulating mechanism for the quick-return mechanism was produced using ProEngineer. The mechanism is shown in Fig. 5.11 and 5.12.

d	0.0021 m
R	0.0069 m
N	27.34

Table 5.5: Parameters of the spring**Figure 5.11:** 3-D model of the modulating mechanism

1.2. Ball Screws. The amplifier should be carefully selected because the torque on the transmission mechanism due to the inertia of the load increases quadratically with the amplification factor. For the same example, if a ball screw with a diameter of 0.0381 m, a lead of 0.0476 m and a length of 3 m is selected, the screw must turn, for a complete stroke of its bolt, through an angle θ given by

$$\theta = \frac{118}{1.875} = 62.93 \text{ revolutions}$$

Using a speed amplifier with an amplification of 1 : 512, the sweep of the follower is calculated to be 44.3°. Note that 512 is the cube of 8, the maximum speed ratio produced with a planar Speed-o-Cam. This ratio is limited by the pressure angle.

1.2.1. Equivalent moment of inertia. The equivalent moment of inertia is induced by all the moving parts coupled to the follower. Again, the inertia on the



Figure 5.12: Front view of the modulating mechanism

follower axis due to the screw, the transported object, and the fixtures, are amplified by a factor of N^2 by the speed amplifier. Therefore, the moment of inertia of the follower and the inertia of the amplifier are neglected, and hence,

$$I_f = (I_s + I_o) \cdot N_{\text{amp}}^2 \quad (5.2)$$

where

I_f : equivalent moment of inertia of the follower;

I_s : moment of inertia of the screw;

I_o : moment of inertia due to the mass of the transported object, and fixtures.

For the ball screw made of stainless steel with density $\rho = 7.92 \times 10^3 \text{ kg/m}^3$,

$$I_s = \frac{\pi}{16} \rho D_p^4 l = 0.0098 \text{ kg m}^2$$

Then,

$$I_f = (0.0098 + 1.12 \times 10^{-4}) \times 512^2 = 2598 \text{ kg m}^2$$

The required torque increases with the square of the amplification; therefore, if a large amplification factor is used, the torque needed to be compensated might not

be feasible. For this example, the fluctuating portion of the torque on the axis of the follower is shown in Fig. 5.13. The maximum torque, of the order of 10^5 Nm, is not achievable with a compact mechanism. Hence, the ball screw is not a feasible U-TSG for this application.

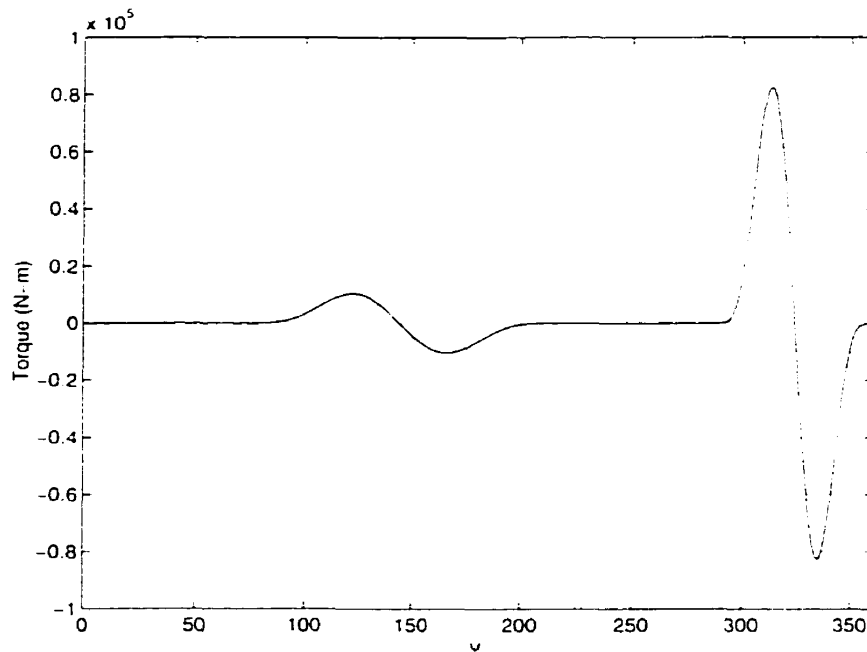


Figure 5.13: Fluctuating torque on the axis of the follower

2. Replacement of Elliptic Gears Using a Single Cam Mechanism

The problem at hand consists of replacing the transmission mechanism of a textile machine, Fig. 5.14, composed of an elliptic-gear train and a four-bar linkage, with a simpler mechanism. The end result is a cam mechanism with minimum size obtained using the method proposed in the previous sections.

The function of the four-bar mechanism is to produce the desired rocker motion of the driven link, whereas the function of the elliptic-gear train is to smooth the motion produced by the four-bar linkage. Indeed, since the motion of the links of

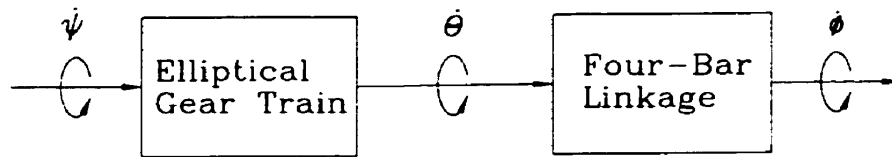


Figure 5.14: Transmission mechanism of a textile machine.

a lower-pair mechanism driven by a uniform speed of its input link is an analytic function (Kreyszig 1988). not all derivatives of the displacement variables can vanish simultaneously. Hence, when the output velocity vanishes, the output acceleration does not, and vice versa. Sketches of the gear train and the four-bar linkage are shown in Figs. 5.15 and 5.16, their parameters being given in Table 5.6.

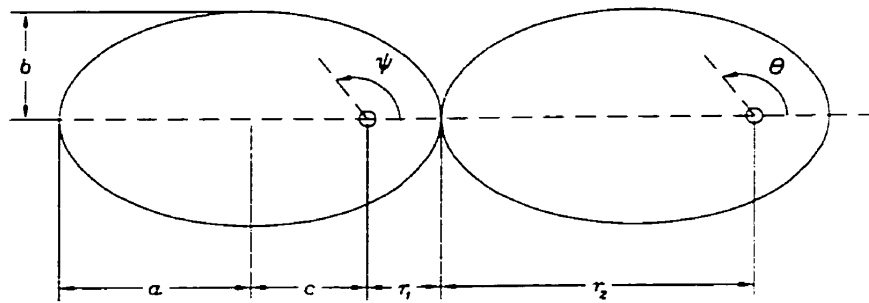


Figure 5.15: Sketch of the elliptic-gear mechanism

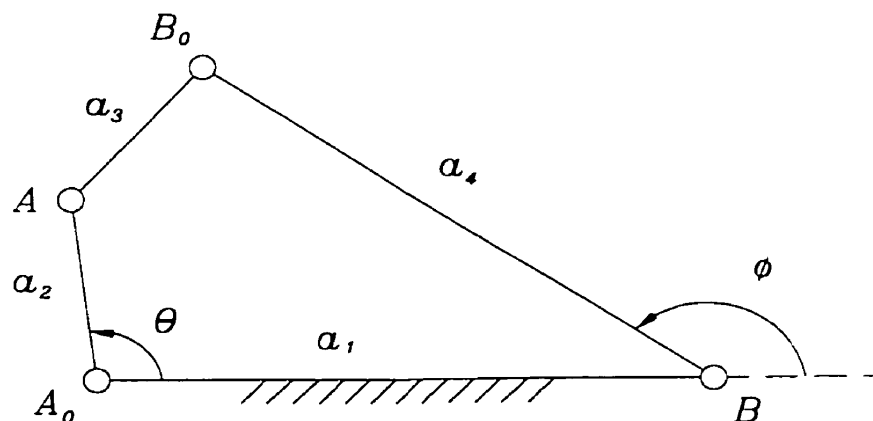


Figure 5.16: Sketch of the four-bar mechanism

Elliptic-gear train		Four-bar linkage	
a	120 mm	a_1	0.84853 m
b	116.49 mm	a_2	0.1 m
c	28.811 mm	a_3	0.17 m
r_1	14.811 mm	a_4	0.84853 m
r_2	91.189 mm		

Table 5.6: Parameters of the transmission mechanism

The input-output functions of the elliptic-gear train (Chironis and Sclater 1996) are

$$\theta(\psi) = \frac{2}{c_3} \tan^{-1} \frac{(c_1 - c_2) \tan\left(\frac{\psi}{2}\right)}{c_3} \quad (5.3a)$$

$$\theta'(\psi) = \frac{1}{c_1 + c_2 \cos(\psi)} \quad (5.3b)$$

$$\theta''(\psi) = \frac{c_2 \sin(\psi)}{(c_1 + c_2 \cos(\psi))^2} \quad (5.3c)$$

where

$$c_1 = \frac{2a^2}{b^2} - 1 \quad (5.4a)$$

$$c_2 = \frac{2ac}{b^2} \quad (5.4b)$$

$$c_3 = \sqrt{c_1^2 - c_2^2} \quad (5.4c)$$

The input-output functions of the four-bar linkage are obtained from the Freudenstein equation (Angeles 1982), namely,

$$k_1 + k_2 \cos \phi - k_3 \cos \theta = \cos(\theta - \phi) \quad (5.5)$$

where

$$k_1 \equiv \frac{a_1^2 + a_2^2 - a_3^2 + a_4^2}{2a_2a_3}, \quad k_2 \equiv \frac{a_1}{a_2}, \quad k_3 \equiv \frac{a_1}{a_4}$$

The velocity and acceleration ratios produced by the four-bar linkage are, in turn,

$$o'(\theta) = \frac{k_3 \sin \theta + \sin(\theta + o)}{k_2 \sin o + \sin(\theta + o)} \quad (5.6a)$$

$$o''(\theta) = \frac{k_3 \cos \theta - o'^2 k_2 \cos o + (1 - o')^2 \cos(\theta - o)}{k_2 \sin o + \sin(\theta - o)} \quad (5.6b)$$

The input output functions of the gear-train, the four-bar linkage, and the composed mechanism are shown in Figures 5.17, 5.18, and 5.19, respectively. The overall input-output function o vs. ψ is shown in Fig. 5.19. The optimum cam mechanism sought must then produce the input output motion of this figure.

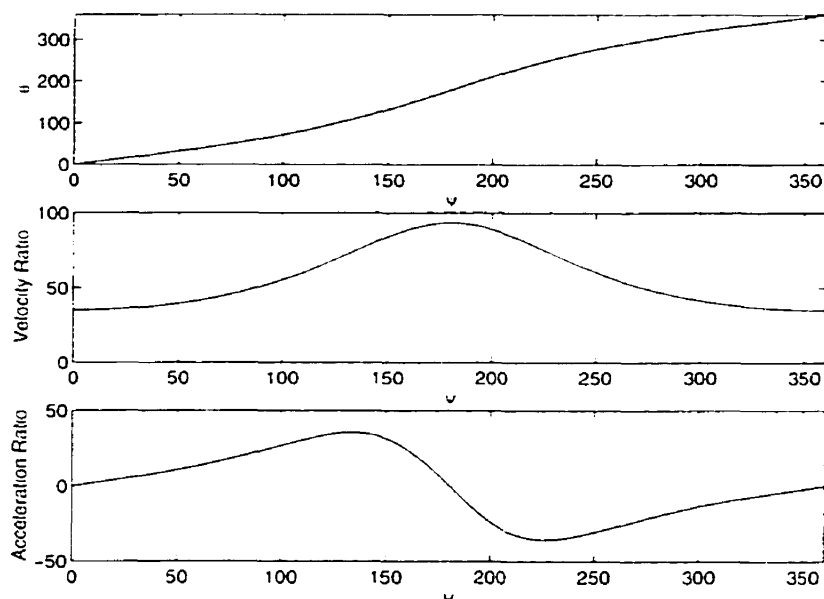


Figure 5.17: Input-output plots of the elliptic-gear train

Several solutions were obtained using the Newton-Raphson method. Some of the solutions are ruled out because they are not feasible: for example, they lead to a negative value of u . The optimum cam mechanism was found to have the parameters shown in Table 5.7.

The pressure-angle distribution of the optimum cam mechanism appears in Fig. 5.20.

5.2 REPLACEMENT OF ELLIPTIC GEARS USING A SINGLE CAM MECHANISM

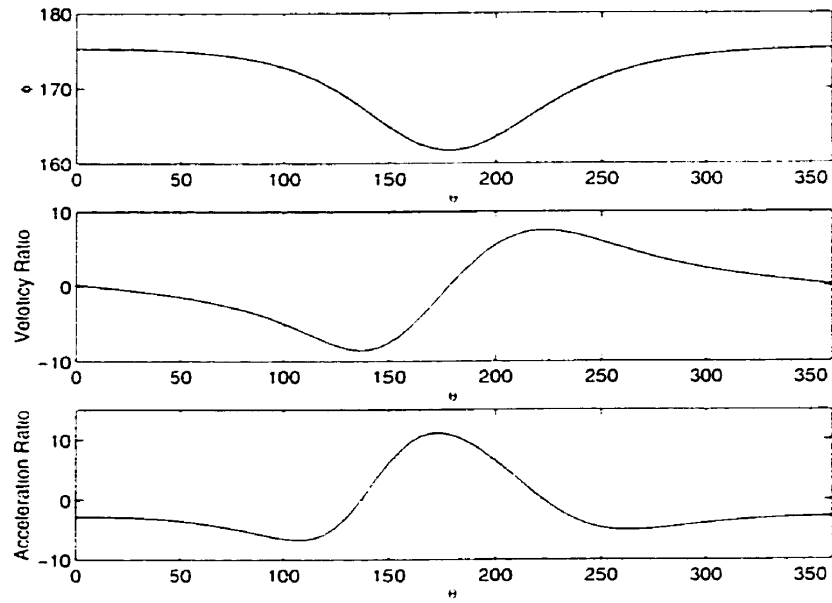


Figure 5.18: Input-output plots of the four-bar linkage

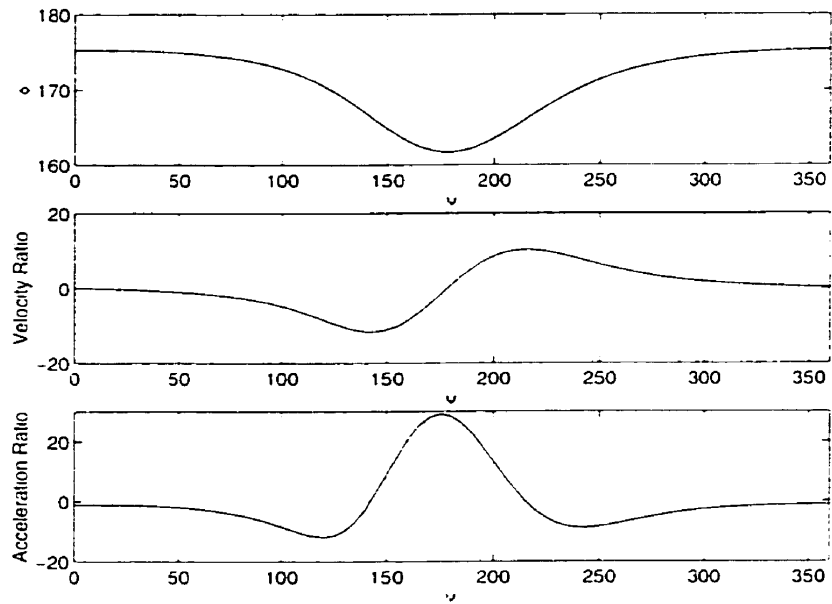


Figure 5.19: Input-output plots of the composed mechanism

5.2 REPLACEMENT OF ELLIPTIC GEARS USING A SINGLE CAM MECHANISM

a	$\beta(\text{rad})$	b	a/l
0.960553	0.257039	0.254304	0.1308

Table 5.7: Parameters of the optimum cam mechanism

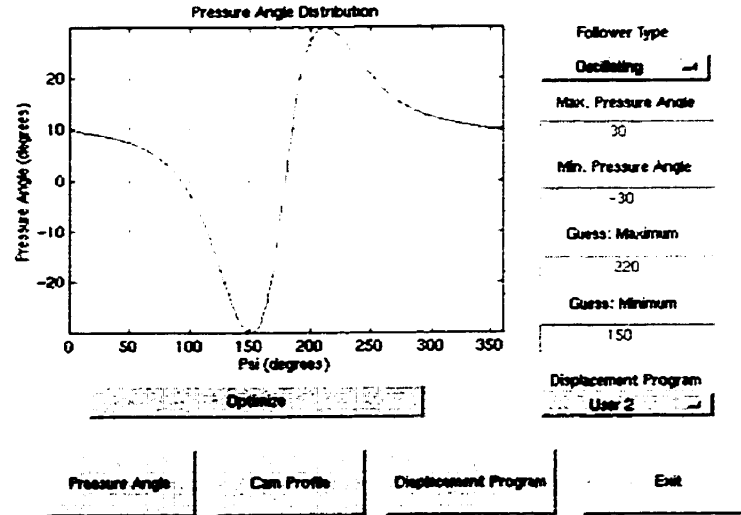


Figure 5.20: Pressure-angle distribution of the optimum cam

To avoid undercutting and with a design factor of 2, the radius of the roller is found to be $a/l = 0.1308$. The cam profile, the pitch-curve, and the base circle are shown in Fig. 5.21.

5.2 REPLACEMENT OF ELLIPTIC GEARS USING A SINGLE CAM MECHANISM

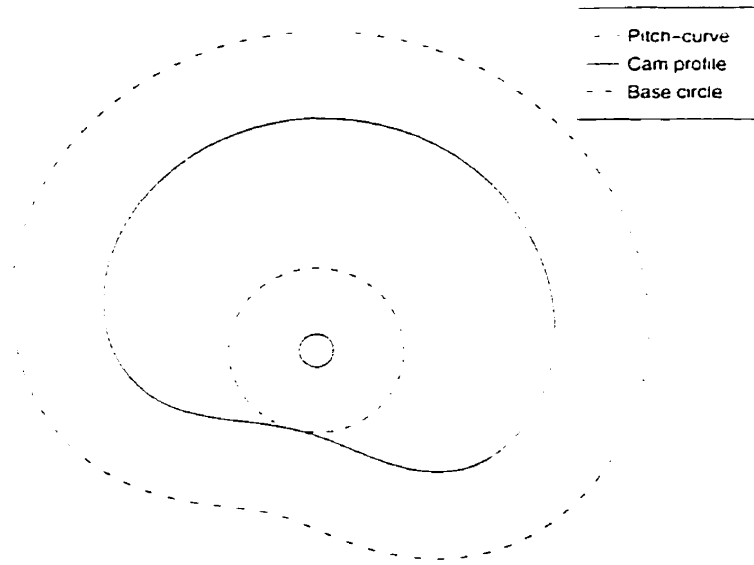


Figure 5.21: Profile of the optimum cam

CHAPTER 6

Conclusions and Recommendations for Future Work

1. Conclusions

A modular approach to the synthesis of quick-return mechanisms is introduced here. Cam mechanisms are used as building blocks in the design of this class of mechanisms. A unified approach to the optimization of cam mechanism is also proposed. The proposed method incorporates additional conditions that guarantee a pressure-angle distribution whereby both the maximum and the minimum attain the allowable extreme values. For translating cam mechanisms the optimization leads to a nonlinear equation of one variable, which can be solved using graphical or numerical methods. For other types of cam mechanisms, the problem leads to a system of nonlinear equations, which can be solved using, e.g., the Newton-Raphson method. A Graphical User Interface to help the designer was developed.

A methodology to synthesize a cam-spring mechanism to compensate the fluctuations of a periodic torque is also introduced. The spring is selected such that resonance due to the reciprocating motion is avoided. The spring of minimum mass is calculated.

A long-stroke, quick-return mechanism needed for a process in the fabrication of veneer strips was optimized using the modular approach. A belt-pulley mechanism

to convert rotary motion to translatory motion and an elastic torque compensator are designed.

The replacement of the transmission mechanism of a textile machine composed of an elliptic-gear train and a four-bar linkage with a simpler mechanism based on cams is also included.

2. Recommendations for Future Work

The proposed optimization method has to be extended to cylindrical, spherical, and spatial cam mechanisms.

Further research is needed to prove that the minimum size of the cam is obtained when the maximum and minimum values of the pressure angle are equal but of opposite signs.

Implementing an optimization method that considers stress concentration when minimizing the cam size should also be given due attention

References

- Angeles, J., 1982. *Spatial Kinematic Chains*. Springer-Verlag, New York.
- Angeles, J., and López-Cajún, C. S., 1991. *Optimization of Cam Mechanisms*. Kluwer-Academic Publishers, Dordrecht.
- Asselin, H., and Doléac, L., 1997. *Conception d'un mécanisme de convoyage à cames*. Technical Report, Ecole Centrale de Nantes, France.
- Berzak, N., 1982. "Optimization of cam-follower systems with kinematic and dynamic constraints". *ASME Journal of Mechanical Design*, Vol. 104, pp. 29-33.
- Bouzakis, K. D., Mitsi, S., and Tsiafis, J., 1997. "Computer-aided optimum design and NC milling of planar cam mechanisms". *International Journal of Machine Tools and Manufacture*, Vol. 37, No. 8, pp. 1131-1142.
- Carlson, H., 1978. *Spring Designer's Handbook*. Marcel Dekker, Inc., New York.
- Chan, Y. W., and Kok, S. S., 1996. "Optimum cam design". *International Journal of Computer Applications in Technology*, Vol. 9, No. 1, pp. 34-47.
- Chen, F. Y., 1982. *Mechanics and Design of Cam Mechanisms*. Pergamon Press, New York.
- Chironis, N. P., Sclater, N., 1996 *Mechanisms and Mechanical Devices Sourcebook*. Second Edition, McGraw-Hill, New York
- Denavit, J. and Hartenberg, R.S., 1964. *Kinematic Synthesis of Linkages*. McGraw-Hill, New York.

- Duffy, J., 1980. *Analysis of Mechanisms and Robot Manipulators*. Edward Arnold, London.
- Erdman, A. G., 1993. *Modern Kinematics: Developments in the Last Forty Years*. John Wiley & Sons, New York.
- González-Palacios, M. A., and Angeles, J., 1993. *Cam Synthesis*. Kluwer-Academic Publishers, Dordrecht.
- González-Palacios, M. A., and Angeles, J., 1998. "The Design of a Novel Mechanical Transmission for Speed Reduction". *ASME Design Engineering Technical Conferences*, Atlanta, September, pp. 13-16
- Hirschhorn, J., 1962. "Pressure angle and minimum base radius". *Machine Design*, Vol. 34, pp. 191-192.
- Jones, J. R., 1978. "Mechanisms: Pressure angles and forces in cams". *Engineering*, Vol. 218, pp. 703-706.
- Koloc, Z., and Václavík, M., 1993. *Cam Mechanisms*. Elsevier, Amsterdam.
- Kreyszig, E., 1988. *Advanced Engineering Mathematics*. John Wiley & Sons, New York.
- Lam, G. H., Teng, C. P., and Angeles, J., 1997. "The synthesis of an elastic torque compensator for a transmission subjected to a periodic load". *The Seventh IFToMM International Symposium on Linkages and Computer Aided Design Methods*, Bucharest, 26-30 August, Vol. 3, pp. 291-298.
- Loeff, L., and Soni, A. H., 1975. "Optimum sizing of planar cams". *Proc. 4th World Congress on Theory of Machines and Mechanisms*, Newcastle upon Tyne, Vol. 4, pp. 777-780.
- Mills, J. K., Notash, L., and Fenton, R. G., 1993. "Optimal design and sensitivity analysis of flexible cam mechanisms". *Mechanisms and Machine Theory*, Vol. 28, No. 4, pp. 563-581.

- Nishioka, M., and Uchino, M., 1993. "Compensation of input shaft torque on indexing cam mechanisms (in Japanese)". *Transactions of the Japan Society of Mechanical Engineers*, Vol. 59, No. 562, pp. 1913-1919.
- Nishioka, M., 1994. "Compensation of input shaft torque on indexing cam mechanisms (2nd report) (in Japanese)". *Transactions of the Japan Society of Mechanical Engineers*, Vol. 60, No. 569, pp. 338-342.
- Nishioka, M., and Yoshizawa, M., 1994. "Compensation of input shaft torque on indexing cam mechanisms (3rd report) (in Japanese)". *Transactions of the Japan Society of Mechanical Engineers*, Vol. 60, No. 576, pp. 2830-2836.
- Nishioka, M., and Yoshizawa, M., 1995. "Direct torque compensation cam mechanisms (1st report) (in Japanese)". *Transactions of the Japan Society of Mechanical Engineers*, Vol. 61, No. 585, pp. 2020-2024.
- Norton, R. L., 1992. *Design of Machinery*, McGraw-Hill, New York.
- Rothbart, H. A., 1956. *Cams. Design, Dynamics, and Accuracy*, John Wiley, New York.
- Spotts, M. F., 1985. *Design of Machine Elements*, Prentice-Hall, New Jersey, Sixth Edition.
- Tesar, D., and Matthew, G. K., 1976. *The Dynamic Synthesis, Analysis, and Design of Modeled Cam systems*, Lexington Books, Massachusetts.
- Wahl, A. M., 1944. *Mechanical Springs*, Penton Publishing, Cleveland.

APPENDIX A

Pitch Curve and Cam Profile

In order to avoid undercutting or large contact-stresses between the cam and the roller, the radius of the roller must be a fraction of the minimum radius of curvature of the pitch curve. The expression for the curvature of the pitch curve is given as (Angeles and López-Cajún, 1991).

$$\kappa = \frac{N}{D} \quad (\text{A.1})$$

where

$$N = e^2 (1 + \phi')^3 - e\ell [(1 + \phi')(2 + \phi') \cos \phi + \phi'' \sin \phi] + \ell^2$$

$$D = [e^2 (1 + \phi')^2 - 2e\ell(1 + \phi') \cos \phi + \ell^2]^{\frac{3}{2}}$$

Therefore, the minimum radius of curvature is

$$r_{\min} = \frac{1}{\kappa_{\max}}$$

The pitch curve of the oscillating cam-follower is generated using the relations (Angeles and López-Cajún 1991)

$$x_p(\psi) = \ell \cos \psi - e \cos(\psi + \phi) \quad (\text{A.2a})$$

$$y_p(\psi) = -\ell \sin \psi + e \sin(\psi + \phi) \quad (\text{A.2b})$$

The cam profile is obtained using the geometry of Fig. A.1, namely,

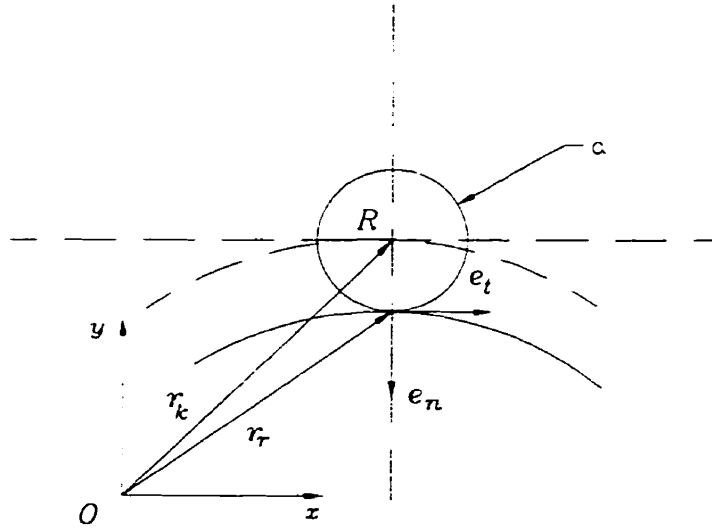


Figure A.1: Geometry of the cam profile.

$$\mathbf{r}_r = \mathbf{r}_k + a\mathbf{e}_n \quad (\text{A.3})$$

where

$$\mathbf{r}_k(\iota) = x_p(\iota)\mathbf{i} + y_p(\iota)\mathbf{j} \quad (\text{A.4a})$$

$$\mathbf{r}'_k(\iota) = x'_p(\iota)\mathbf{i} + y'_p(\iota)\mathbf{j} \quad (\text{A.4b})$$

$$\mathbf{e}_n = \frac{y'_p}{\|\mathbf{r}'_k\|}\mathbf{i} - \frac{x'_p}{\|\mathbf{r}'_k\|}\mathbf{j} \quad (\text{A.4c})$$

Therefore, $\mathbf{r}_r(\iota) = x(\iota)\mathbf{i} + y(\iota)\mathbf{j}$, where

$$x(\iota) = x_p(\iota) + a\frac{y'_p(\iota)}{\|\mathbf{r}'_k\|} \quad (\text{A.5a})$$

$$y(\iota) = y_p(\iota) - a\frac{x'_p}{\|\mathbf{r}'_k\|} \quad (\text{A.5b})$$